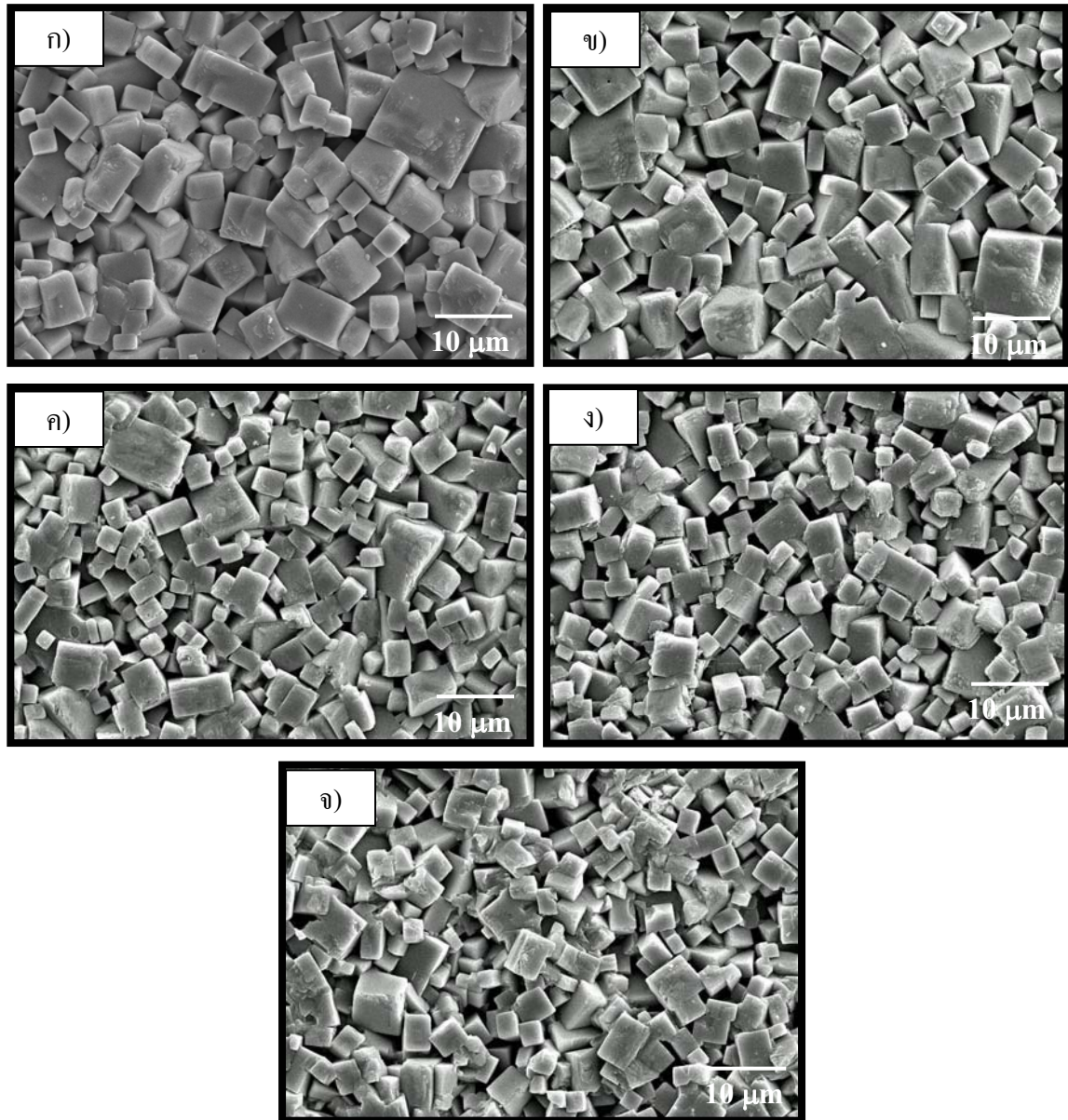
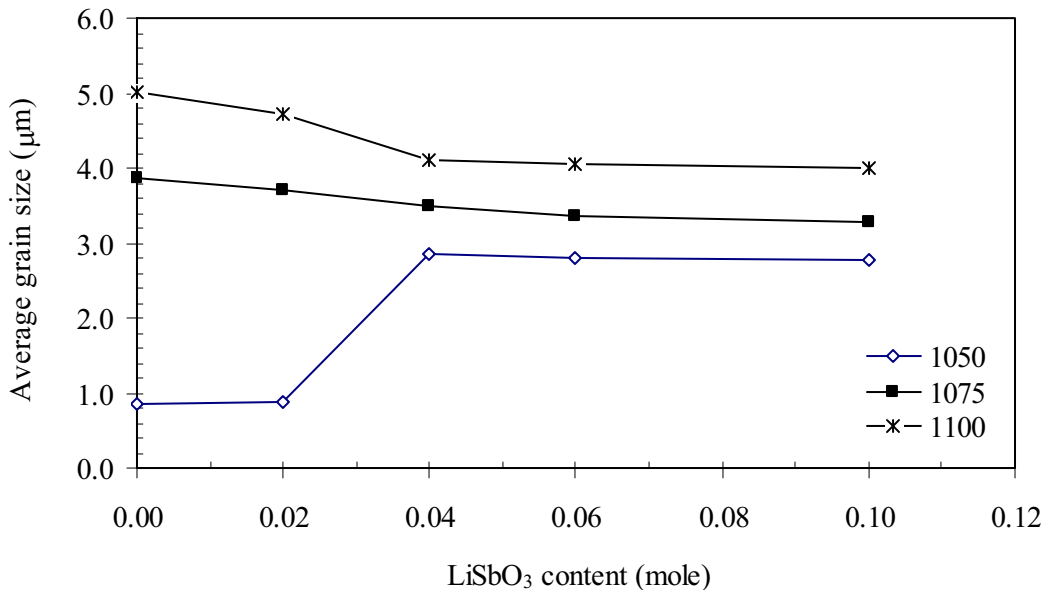


รูป 3.41 ภาพถ่าย SEM ของเซรามิก  $(0.95-n)(Na_{0.5}K_{0.5})NbO_3 - 0.05 LiTaO_3 - n LiSbO_3$  เมื่อ ชินเตอร์ที่อุณหภูมิ  $1075^{\circ}C$



รูป 3.42 ภาพถ่าย SEM ของเซรามิก  $(0.95-n)(Na_{0.5}K_{0.5})NbO_3 - 0.05 LiTaO_3 - n LiSbO_3$  เมื่อ ชินเตอร์ที่อุณหภูมิ  $1100^{\circ}C$



รูป 3.43 ขนาดกรานเฟลี่ยของเซรามิก  $(0.95-n)(\text{Na}_{0.5}\text{K}_{0.5})\text{NbO}_3 - 0.05 \text{ LiTaO}_3 - n \text{ LiSbO}_3$  เมื่อ ชิ้นเตอร์ที่อุณหภูมิต่างๆ กัน

### 3.2.6.4 การตรวจสอบสมบัติทางไฟฟ้าของเซรามิกในระบบ $(0.95-n)(\text{Na}_{0.5}\text{K}_{0.5})\text{NbO}_3 - 0.05 \text{ LiTaO}_3 - n \text{ LiSbO}_3$

#### 3.2.6.4.1 ค่าคงที่ไดอิเล็กตริก

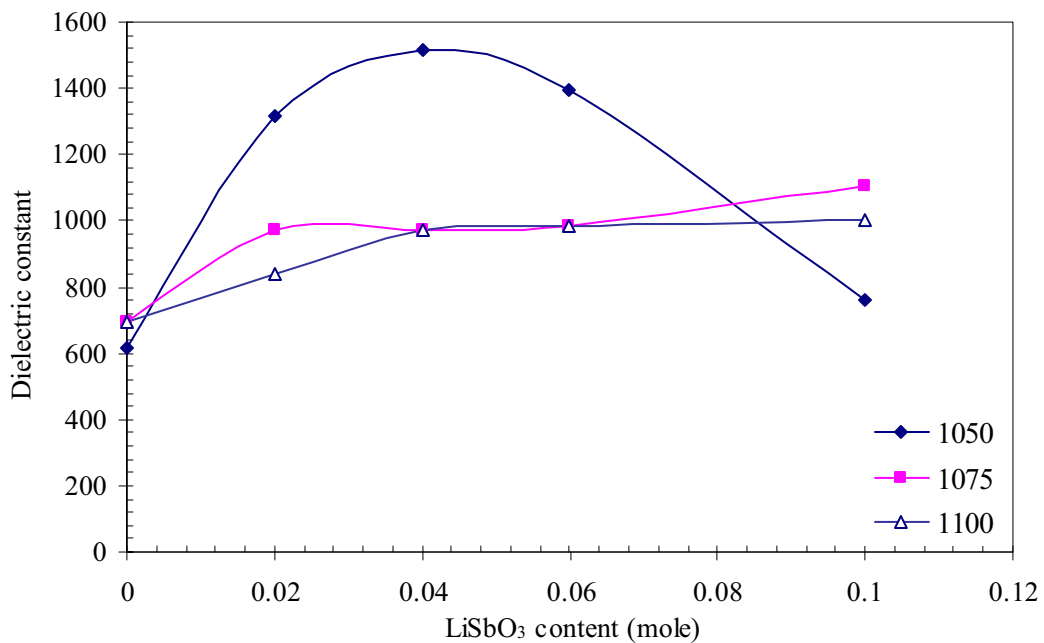
เมื่อพิจารณาค่าคงที่ไดอิเล็กตริก (dielectric constant,  $\epsilon_r$ ) และแฟกเตอร์การสูญเสียในรูป ของความร้อน (dissipation factor,  $\tan \delta$ ) ของสารตัวอย่าง ดังแสดงในรูป 3.44 – 3.45 พบว่า ทั้ง  $\epsilon_r$  และ  $\tan \delta$  มีค่าขึ้นอยู่กับสัดส่วนค่า  $n$  และอุณหภูมิชิ้นเตอร์เป็นอย่างมาก โดยสารตัวอย่างเมื่อ  $n = 0.0$  (NKN-LT) ให้ค่า  $\epsilon_r$  อยู่ในช่วง 600 – 700 สำหรับการชิ้นเตอร์ในช่วง 1050 – 1100 °C ซึ่งค่าที่ได้นี้เมื่อ นำไปเปรียบเทียบกับงานวิจัยอื่นๆ [41] พบว่า มีค่าสูงกว่าเล็กน้อยและเมื่อเปรียบเทียบกับเซรามิก  $(\text{Na}_{0.5}\text{K}_{0.5})\text{NbO}_3$  ในงานวิจัยนี้ พบว่า NKN-LT ให้ค่าต่ำกว่าเล็กน้อย อย่างไรก็ตาม ค่า  $\epsilon_r$  ที่ได้จากระบบ นี้มีค่าสูงกว่าเซรามิก  $(\text{Na}_{0.5}\text{K}_{0.5})\text{NbO}_3$  ในงานวิจัยของ Guo, และคณะ [10] มาก ซึ่งมีค่าประมาณ 400

สำหรับสารตัวอย่างที่เติม  $\text{LiTaO}_3$  ( $n = 0.02-0.10$ ) พบว่า ค่า  $\epsilon_r$  มีค่าสูงขึ้น โดยสารตัวอย่าง เมื่อ  $n = 0.04$  ให้ค่า  $\epsilon_r$  สูงสุดประมาณ 1510 เมื่อชินเตอร์ที่อุณหภูมิ  $1050^\circ\text{C}$  และสารตัวอย่างเมื่อ  $n = 0.02$  และ  $0.06$  ให้ค่าสูงเท่านั้น โดยอยู่ในช่วง  $1300 - 1350$  แต่สำหรับสารตัวอย่างเมื่อ  $n = 0.10$  ค่าที่ได้กลับมีค่าลดลงและใกล้เคียงกับสารตัวอย่างเมื่อ  $n = 0.0$  (รูป 3.44) ทั้งนี้เนื่องจากการมี  $\text{LiSbO}_3$  ที่ยังทำปฏิกิริยาไม่สมบูรณ์หลังเหลืออยู่ (รูป 3.35)

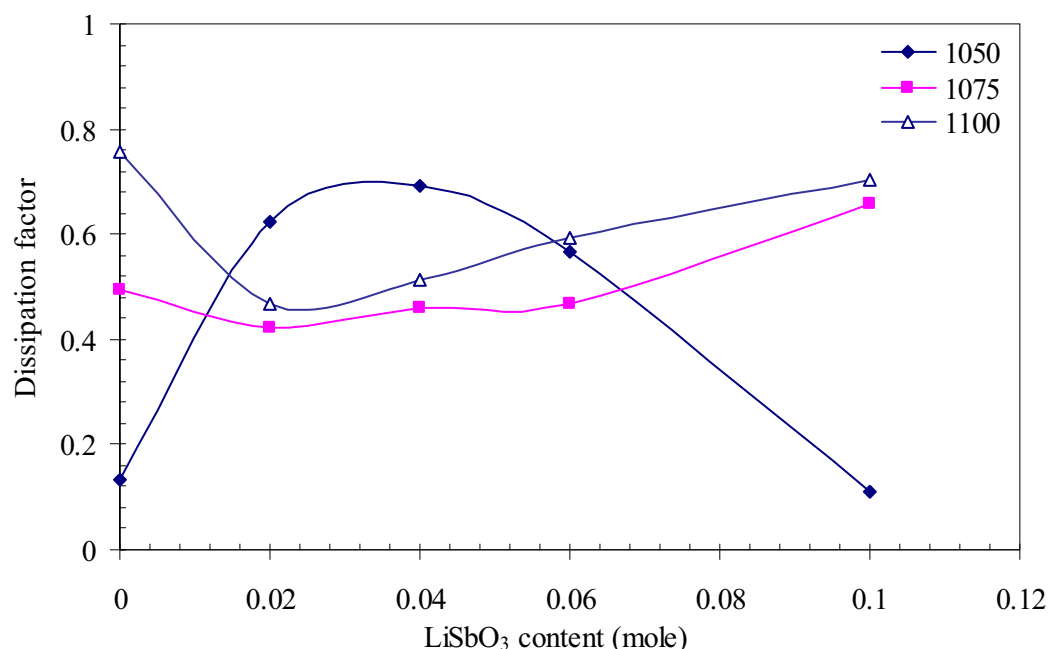
การมีค่า  $\epsilon_r$  สูงประมาณ 1510 ในสารตัวอย่างเมื่อ  $n = 0.04$  เมื่อนำไปเปรียบเทียบงานของ Saito และคณะ ซึ่งเตรียมสาร  $(\text{K}_{0.44}\text{Na}_{0.52}\text{Li}_{0.04})(\text{Nb}_{0.86}\text{Ta}_{0.10}\text{Sb}_{0.04})\text{O}_3$  ด้วยวิธี reactive grain growth (RTGG) ซึ่งมีลักษณะเกรนแบบเทกเตอร์ (textured) [14] และเป็นลักษณะที่มีรายงานว่าจะให้ค่าสมบัติทางไฟฟ้าที่ดี พบว่า มีค่าอยู่ในช่วงเดียวกัน ซึ่งสามารถสรุปได้ว่า การเติมสารเจือทั้ง  $\text{LiTaO}_3$  และ  $\text{LiSbO}_3$  ร่วมกัน และเตรียมด้วยวิธีชินเตอร์แบบปกติ ส่งผลให้สารตัวอย่างมีสมบัติโดยอิเล็กทริกที่ดีเทียบเท่ากับการเตรียมด้วยวิธี RTGG

เมื่อพิจารณาการชินเตอร์ที่อุณหภูมิสูงขึ้น ( $1075$  หรือ  $1100^\circ\text{C}$ ) พบว่า ค่า  $\epsilon_r$  ที่ได้มีค่าลดลง และต่ำกว่าสารตัวอย่างที่ชินเตอร์ที่อุณหภูมิ  $1050^\circ\text{C}$  โดยมีค่าอยู่ในช่วง  $800 - 1000$  สำหรับทุกตัวอย่าง

สำหรับค่า  $\tan \delta$  ของสารตัวอย่างเมื่อเติม  $\text{LiSbO}_3$  พบว่ามีค่าสูงประมาณ  $0.1 - 0.7$  โดยค่าสูงที่สุดพบในสารตัวอย่างที่ให้ค่า  $\epsilon_r$  สูงสุด และสำหรับสารตัวอย่างที่ไม่เติม  $\text{LiSbO}_3$  ค่า  $\tan \delta$  มีค่าเพิ่มขึ้นตามอุณหภูมิชินเตอร์ที่เพิ่มขึ้น (รูป 3.45) ซึ่งค่า  $\tan \delta$  ที่สูงนี้อาจเนื่องมาจากการมีสภาพนำไฟฟ้าที่สูงของสารตัวอย่างซึ่งเกิดมาจากการสูญเสียออกไซด์พวกลอคลาไลน์ในระหว่างการชินเตอร์



รูป 3.44 ค่าคงที่ไดอิเล็กตริกของเซรามิก  $(0.95-n)(Na_{0.5}K_{0.5})NbO_3 - 0.05 LiTaO_3 - n LiSbO_3$  เมื่อชิ้นเตอร์ที่อุณหภูมิต่างๆ กัน



รูป 3.45 แฟกเตอร์การสูญเสียในรูปของความร้อนของเซรามิก  $(0.95-n)(Na_{0.5}K_{0.5})NbO_3 - 0.05 LiTaO_3 - n LiSbO_3$  เมื่อชิ้นเตอร์ที่อุณหภูมิต่างๆ กัน

### 3.2.6.4.2 ค่า $d_{33}$

สำหรับสารตัวอย่างในระบบนี้ได้เลือกสารตัวอย่างที่มีค่าไดโอดิลีกตริกสูงสุดมาวัดค่า  $d_{33}$  พบว่า มีค่าประมาณ 170 pC/N ซึ่งเป็นค่าที่สูงพอสมควรและสามารถนำไปประยุกต์งานทางค้านอัลตราโซนิกส์ อย่างไรก็ตาม ค่าที่ได้ยังมีค่าน้อยกว่าในงานวิจัยของ Saito และคณะ ซึ่งมีค่าประมาณ 300 pC/N เมื่อศึกษาระบบ  $(K_{0.44}Na_{0.52}Li_{0.04})(Nb_{0.86}Ta_{0.10}Sb_{0.04})O_3$  ด้วยวิธีการเตรียมแบบเดียวกัน และค่า  $d_{33}$  มีค่าประมาณ 416 pC/N เมื่อเตรียมด้วยวิธี reactive grain growth (RTGG) [14]

## 4. สรุปผลการวิจัยและข้อเสนอแนะ

### 4.1 สรุปผลการวิจัย

#### 4.1.1 การเตรียมผง ( $Na_{1-x}K_xNbO_3$ )

การเตรียมผงสารตัวอย่าง ( $Na_{1-x}K_xNbO_3$ ) เมื่อ  $x = 0.2, 0.4, 0.5, 0.6$  และ  $0.8$  ด้วยวิธีสมอกราฟฟิคแบบที่ใช้กันทั่วไป และใช้  $Na_2CO_3$ ,  $K_2CO_3$  และ  $Nb_2O_5$  เป็นสารตั้งต้น พบว่า สารตัวอย่างเกิดการฟอร์มตัวเป็นผลึกที่มีสมมาตรแบบออร์โธรอมบิกได้ดีเมื่อเผาที่อุณหภูมิ  $900^{\circ}C$  เป็นเวลานาน 2 ชั่วโมง สำหรับ  $x = 0.2, 0.4$  และ  $0.8$  และที่อุณหภูมิ  $900^{\circ}C$  เป็นเวลานาน 6 ชั่วโมง สำหรับ  $x = 0.5$  และสำหรับ  $x = 0.6$  จะต้องใช้อุณหภูมิที่สูงกว่า  $900^{\circ}C$  เป็นเวลานาน 2 ชั่วโมง จึงจะทำให้ได้สารตัวอย่างที่บริสุทธิ์ เนื่องจากยังมีพิคของ  $K_2CO_3$  ปรากฏอยู่ นอกจากนี้ ได้ศึกษาผลของการเติมสารตั้งต้นประเภทการ์บอนเนตส่วนเกิน ( $Na_2CO_3$  และ  $K_2CO_3$ ) ในสารตัวอย่างเมื่อ  $x = 0.5$  พบว่าเมื่อเติมสารตั้งต้นในปริมาณที่เพิ่มขึ้นประมาณ 0.05 โมล จะสามารถลดอุณหภูมิในการแคลไชน์ให้ต่ำลงได้ คือ จะเกิดการฟอร์มเป็นผลึกที่มีสมมาตรแบบออร์โธรอมบิกได้อย่างสมบูรณ์เมื่อเผาแคลไชน์ที่อุณหภูมิ  $800^{\circ}C$  เป็นเวลานาน 2 ชั่วโมง

สำหรับลักษณะรูปร่างและขนาดของอนุภาคน้ำที่ขึ้นอยู่กับสัดส่วนของค่า  $x$  ปริมาณสารตั้งต้นประเภทการ์บอนเนตส่วนเกิน อุณหภูมิและเวลาที่ใช้ในการแคลไชน์ ทั้งนี้ขึ้นอยู่กับของอนุภาคน้ำที่มากขึ้นเมื่ออุณหภูมิและเวลาแคลไชน์มากขึ้นหรือปริมาณสารตั้งต้นส่วนเกินเพิ่มขึ้น โดยอนุภาคน้ำโดยที่สุดประมาณ  $1.0 - 2.5 \mu m$  และมีรูปร่างเป็นทรงสี่เหลี่ยมพจน์ในสารตัวอย่าง ( $Na_{0.5}K_{0.5}NbO_3$ ) ที่เติมสารตั้งต้นประเภทการ์บอนเนตส่วนเกินปริมาณ 0.05 โมล และเผาแคลไชน์ที่อุณหภูมิ  $900^{\circ}C$  เป็นเวลา 2 ชั่วโมง

#### 4.1.2 การเตรียมเซรามิก ( $Na_{1-x}K_xNbO_3$ )

สำหรับการเตรียมเซรามิก ที่ค่า  $x$  ต่างๆ และ ( $Na_{0.5}K_{0.5}NbO_3$ ) ที่เจือด้วยสารเจือชนิดต่างๆ คือ สารตั้งต้นประเภทการ์บอนเนตส่วนเกิน,  $LiTaO_3$ ,  $BaTiO_3$  และ  $LiTaO_3$  ปริมาณ 0.05 โมล ผสมกับ  $LiSbO_3$  ในปริมาณต่างๆ กัน โดยเผาแคลไชน์ที่อุณหภูมิ  $900^{\circ}C$  เป็นเวลา 2 ชั่วโมง (ยกเว้น ( $Na_{0.5}K_{0.5}NbO_3$ ) ที่เติม  $K_2CO_3$  และ  $Na_2CO_3$  ส่วนเกิน ปริมาณ 0.05 โมล และเติม  $LiTaO_3$  ปริมาณ 0.05 โมล ผสมกับ  $LiSbO_3$  ในปริมาณต่างๆ เผาแคลไชน์ที่อุณหภูมิ  $800^{\circ}C$  เป็นเวลา 2 ชั่วโมง) เผาเซ็นเตอร์ที่อุณหภูมิต่างๆ ในช่วง  $1000 - 1200^{\circ}C$  เป็นเวลา 2 ชั่วโมง ด้วยอัตราการขึ้น/ลงของอุณหภูมิ  $5^{\circ}C$  ต่อนาที พบว่า แนวโน้มของอุณหภูมิซินเตอร์จะสูงขึ้น เมื่ออัตราส่วนของ  $x$ , ปริมาณ  $BaTiO_3$  และปริมาณสารตั้งต้นประเภทการ์บอนเนตส่วนเกินมีค่าเพิ่มขึ้น และแนวโน้มของอุณหภูมิซินเตอร์จะลดลง เมื่อเติม

$\text{LiTaO}_3$  ปริมาณเพิ่มขึ้น และจากการทดสอบสมบัติทางกายภาพของสารตัวย่าง พบว่า ความหนาแน่น การหดตัว และโครงสร้างจุลภาคจะมีค่าขึ้นอยู่กับอุณหภูมิชินเตอร์, ค่า  $x$ , ชนิดและปริมาณของสารเจือ และปริมาณสารตั้งต้นประเภทคาร์บอนเนตส่วนเกิน สำหรับโครงสร้างผลึกของสารตัวอย่างนั้นไม่เกิด การเปลี่ยนแปลงโดยมีลักษณะสมมาตรแบบออร์โธรอมบิก เมื่อเจือด้วยสารตั้งต้นประเภทคาร์บอนเนต ส่วนเกิน และ  $\text{LiTaO}_3$  ปริมาณ  $0.00 - 0.06$  โนมล แต่จะเปลี่ยนเป็นแบบคิวบิกเมื่อเจือ  $\text{BaTiO}_3$  และมีทั้ง แบบออร์โธรอมบิกร่วมกับเตตระโภนอลเมื่อเจือด้วย  $\text{LiTaO}_3$  และ  $\text{LiSbO}_3$  เมื่อชินเตอร์ที่อุณหภูมิ  $1050^{\circ}\text{C}$  อย่างไรก็ตาม จะมีเฟสปนเปี้ยนเกิดขึ้นด้วยดังนี้

- เฟส  $\text{K}_3\text{Li}_2\text{Nb}_5\text{O}_{15}$  ในกรณีที่เจือด้วย  $\text{LiTaO}_3$  ปริมาณ  $0.06$  โนมล ขึ้นไป
- เฟส  $\text{Ba}_{1.31}\text{Ti}_8\text{O}_{16}$  หรือเฟส  $\text{Ba}_{1.07}\text{Ti}_8\text{O}_{16}$  ในกรณีที่เจือด้วย  $\text{BaTiO}_3$  ปริมาณ  $0.06$  โนมล ขึ้นไป
- เฟส  $\text{K}_6\text{Li}_4\text{Nb}_{10}\text{O}_{30}$  ในกรณีที่เติม  $\text{LiTaO}_3$  ปริมาณ  $0.05$  โนมล และ  $\text{LiSbO}_3$  ปริมาณ  $0.0 - 0.10$  โนมล
- เฟส  $\text{LiSbO}_3$  หลังเหลืออยู่ เมื่อเติม  $\text{LiTaO}_3$  ปริมาณ  $0.05$  โนมล และ  $\text{LiSbO}_3$  ปริมาณ  $0.10$  โนมล

สำหรับสมบัติทางไฟฟ้าของสารตัวอย่าง พบว่ามีค่าขึ้นอยู่กับอุณหภูมิชินเตอร์ สัดส่วนค่า  $x$  ชนิดและปริมาณสารเจือ ดังนี้

- สารตัวอย่างเมื่อ  $x = 0.5$  ให้ค่า  $\epsilon_r$  สูงสุดประมาณ  $896$  เมื่อชินเตอร์ที่อุณหภูมิ  $1100^{\circ}\text{C}$
- สารตัวอย่างที่เติมสารตั้งต้นประเภทคาร์บอนเนตส่วนเกินปริมาณ  $0.01$  โนมล ให้ค่า  $\epsilon_r$  สูงสุดประมาณ  $1707$  เมื่อชินเตอร์ที่อุณหภูมิ  $1100^{\circ}\text{C}$
- สารตัวอย่างที่เติม  $\text{LiTaO}_3$  ปริมาณ  $0.02$  โนมล ให้ค่า  $\epsilon_r$  สูงสุดประมาณ  $1241$  เมื่อชินเตอร์ที่อุณหภูมิ  $1100^{\circ}\text{C}$
- สารตัวอย่างที่เติม  $\text{BaTiO}_3$  ปริมาณ  $0.06$  โนมล ให้ค่า  $\epsilon_r$  สูงสุด ประมาณ  $1293$  เมื่อชินเตอร์ที่อุณหภูมิ  $1175^{\circ}\text{C}$
- สารตัวอย่างที่เติม  $\text{LiTaO}_3$  ปริมาณ  $0.05$  โนมล และ  $\text{LiSbO}_3$  ปริมาณ  $0.04$  โนมล ให้ค่า  $\epsilon_r$  สูงสุดประมาณ  $1510$  เมื่อชินเตอร์ที่อุณหภูมิ  $1050^{\circ}\text{C}$

อย่างไรก็ตาม สารตัวอย่างที่เตรียมได้ยังมีค่า  $\tan \delta$  ค่อนข้างสูง ยกเว้นสารตัวอย่างที่เจือด้วย  $\text{BaTiO}_3$  จะให้ค่านี้ค่อนข้างต่ำ โดยจะมีค่าประมาณ  $0.088$

สำหรับค่า  $d_{33}$  ของสารตัวอย่างที่เตรียมได้มีค่าสูงสุด 170 pC/N ซึ่งพบในสารตัวอย่างที่เติม  $\text{LiTaO}_3$  ปริมาณ 0.05 โมล และ  $\text{LiSbO}_3$  ปริมาณ 0.04 โมล สำหรับสารตัวอย่างตัวอื่นๆ พบว่ามีค่าต่ำกว่า 100 pC/N

#### 4.2 ข้อเสนอแนะ

- 4.2.1 สารในระบบมีจุดเหลวค่อนข้างต่ำ จึงควรศึกษาหาตัวเติมเพื่อช่วยลดอุณหภูมิชินเตอร์ให้ต่ำลง เพื่อช่วยป้องกันการสูญเสียของออกไซด์ประเภทอัลคาไลน์
- 4.2.2 ทดลองใช้เครื่องบดผสมสารพลังงานสูง เพื่อจะช่วยให้ได้ค่าความหนาแน่นที่สูงขึ้น
- 4.2.3 เนื่องจากสมบัติทางไฟฟ้านิค่าขึ้นอยู่กับอุณหภูมิชินเตอร์ ดังนั้น จึงควรวัดค่าทุกอุณหภูมิ

## ເອກສາຣອ້າງອີງ

1. Jaffe B, Cook W R, Jaffe H. *Piezoelectric Ceramics*. Academic press, New York, 1971, pp. 185 – 212.
2. Waanders J W, *Piezoelectric Ceramics-Properties and Applications*. Philips Component, Eindhoven, 1991.
3. Maeder M D, Damjanovic D, Setter N. Lead Free Piezoelectric materials, *J Electroceram* 2004; 13 : 385 – 392.
4. Cross E. Materials science: Lead-free at last. *Nature* 2004; 432 : 24-25.
5. Singh K, Lingwal V, Bhatt S C, Panwar, Semwal B S. Dielectric properties of potassium sodium niobate mixed system. *Mater Res Bull* 2001; 36 : 2365 – 2374.
6. Wang R, Xie R, Sekiya T, Shimojo. Fabrication and characterization of potassium-sodium niobate piezoelectric ceramics by spark-plasma-sintering method. *Mater Res Bull* 2004; 39 : 1709 – 1715.
7. Tashiro S, Nagata K. Influence of Mixing condition and nonstoichiometry on piezoelectric properties of (K, Na, Pb)NbO<sub>3</sub> ceramics. *Jpn J App Phys* 2004; 43[9B] : 6711 – 6715.
8. Ichiki M, Zhang L, Tanaka M, Maeda R. Electrical properties of piezoelectric sodium-potassium niobate. *J Eur Ceram Soc* 2004; 24 : 1693 – 1697.
9. Guo Y, Kakimoto K-I, Ohsato H. Dielectric and piezoelectric properties of lead-free (Na<sub>0.5</sub>K<sub>0.5</sub>)NbO<sub>3</sub> – SrTiO<sub>3</sub> ceramics. *Solid State Commun* 2004; 129 : 279 – 284.
10. Guo Y, Kakimoto K-I, Ohsato H. (Na<sub>0.5</sub>K<sub>0.5</sub>)NbO<sub>3</sub> – LiTaO<sub>3</sub> lead-free piezoelectric ceramics. *Mater Lett* 2005; 59 : 241-244.
11. Park S-H, Ahn C-W, Nahm S, Song J-S. Microstructure and piezoelectric properties of ZnO-added (Na<sub>0.5</sub>K<sub>0.5</sub>)NbO<sub>3</sub> ceramics. *Jpn J Applied Phys* 2004; 43[8B] : L1072 – L1074.
12. Guo Y, Kakimoto K-I, Ohsato H. Structure and electric properties of lead-free (Na<sub>0.5</sub>K<sub>0.5</sub>)NbO<sub>3</sub> – BaTiO<sub>3</sub> ceramics. *Jpn J Applied Phys* 2004; 43[9B] : 6662 – 6666.
13. Matsubara M, Yamaguchi Y, Kikuta K, Hirano S-I. Sinterability and piezoelectric properties of (K, Na)NbO<sub>3</sub> ceramics with novel sintering aid. *Jpn J Applied Phys* 2004; 43[10] : 7159 – 7163.

14. Saito Y, Takao H, Tani T, Nonoyama T, Takatori K, Homma T, Nagaya T, Nakamura M. Lead-free piezoelectrics. *Nature* 2004; 84 - 87.
15. Matsubara M, Yamaguchi T, Sakamoto W, Kikuta K, Yogo T, Hirano S -I. Processing and piezoelectric properties of lead-free  $(K, Na)(Nb, Ta)O_3$  ceramics. *J Am Ceram Soc* 2005; 88[5] : 1190 – 1196.
16. Hollenstein E, Davis M, Damjanovic D, Setter N. Piezoelectric properties of Li - and Ta – modified  $(K_{0.5}Na_{0.5})NbO_3$  ceramics. *App Phys Lett* 2005; 87 : 182905.
17. Zhen Y, Li J-F. Normal sintering of  $(K, Na)NbO_3$ -based ceramics: influence of sintering temperature on densification, microstructure, and electrical properties. *J Am Ceram Soc* 2006; 88[12] : 3669 - 3675.
18. Saito Y, Takao H. High performance lead-free piezoelectric ceramics in the  $(K, Na)NbO_3$  –  $LiTaO_3$  solid solution system. *Ferroelectrics* 2006; 338 : 17 - 32.
19. Yoo J, Lee K, Chung K, Lee S, Kim K. Piezoelectric and dielectric properties of  $(LiNaK)(NbTaSb)O_3$  ceramics with variation in poling temperature. *Jpn App Phys* 2006; 45[9B] : 7444 – 7448.
20. Du H, Li Z, Fusheng T, Qu S, Pei Z, Zhou W. Preparation and piezoelectric properties of  $(K_{0.5}Na_{0.5})NbO_3$  lead-free piezoelectric ceramics with pressure-less sintering. *Mater Sci Eng B* 2006; 131 : 83 – 87.
21. Chang Y, Yang Z, Wei L, Liu B. Effects of  $AETiO_3$  additions on phase structure, microstructure and electrical properties of  $(K_{0.5}Na_{0.5})NbO_3$  ceramics. *Mater Sci Eng A* 2006; in press.
22. Zuo R, RÖdel J, Chen R, Li L. Sintering and electrical properties of lead-free  $Na_{0.5}K_{0.5}NbO_3$  piezoelectric ceramics. *J. Am Ceram Soc* 2006; 89[6] : 2010 – 2015.
23. Takao H, Saito Y, Aoki Y, Horibuchi K. Microstructural evolution of crystalline-oriented  $(K_{0.5}Na_{0.5})NbO_3$  piezoelectric ceramics with a sintering aids of Cuo. *J. Am Ceram Soc* 2006; 89[6] : 1951 - 1956.
24. Pettry J-R G, Saïd S, Marchet P, Mercurio J-P. Sodium-bismuth titanate based lead-free ferroelectric materials. *J. Eur Ceram Soc* 2004; 24 : 1165 - 1169.
25. Hao X, Yang Y F. The dielectric and ferroelectric properties of tungsten bronze ferroelectric  $(K_{0.5}Na_{0.5})_{0.1}(Sr_{0.5}Ba_{0.5})_{0.95}Nb_2O_6$  ceramic. *J Mater Sci* 2007; 42 : 3276 – 3279.

26. Raghavender M, Kumar G S, Prasad G. Dispersion of relaxation time in impedance measurements of  $\text{Na}_{1-x}\text{K}_x\text{NbO}_3$  mixed ceramic. *Ferroelectrics* 2005; 324 : 43 – 47.

27. Li J-F, Wang K, Zhang B-P, Zhang L-M. Ferroelectric and piezoelectric properties of fine-grained  $\text{Na}_{0.5}\text{K}_{0.5}\text{NbO}_3$  lead-free piezoelectric ceramics prepared by spark plasma sintering. *J. Am Ceram Soc* 2006; 89[2] : 706 - 709.

28. Cross L E. Electric Double Hysteresis in  $(\text{K}_x\text{Na}_{1-x})\text{NbO}_3$  Single Crystals. *Nature* 1958; 181 : 178 - 179.

29. Ringgaard E, Wurlitzer T. Lead-free piezoceramics based on alkali niobates. *J. Eur Ceram Soc* 2005; 25 : 2701 - 2706.

30. Egerton L, Dillon D D. Piezoelectric and dielectric properties of ceramics in the system potassium-sodium niobate. *J. Am Ceram Soc* 1959; 42[9] : 438 - 442.

31. Jaeger R E, Egerton L. Hot pressing of potassium-sodium niobates. *J. Am Ceram Soc* 1962; 45[5] : 209 - 213.

32. Haerting G H. Properties of hot-pressed ferroelectric alkali niobate ceramics. *J. Am Ceram Soc* 1967; 50[6] : 329 - 330.

33. Du H, Tang F, Luo F, Zhou W, Qu S, Pei Z. Effect of poling condition on piezoelectric properties of  $\text{Na}_{0.5}\text{K}_{0.5}\text{NbO}_3$ - $\text{LiNbO}_3$  lead-free piezoelectric ceramics. *Mater Sci Eng B* 2007; 137 : 175 -179.

34. Du H, Tang F, Luo F, Zhu D, Qu S, Pei Z, Zhou W. Influence of sintering temperature on piezoelectric properties of  $\text{Na}_{0.5}\text{K}_{0.5}\text{NbO}_3$ - $\text{LiNbO}_3$  lead-free piezoelectric ceramics. *Mater Res Bull* 2007; in press.

35. Askeland D R. *The Science and Engineering of Materials*. Chapman & Hall, London, 1996, pp. 67 -68.

36. Lingwal V, Semwal B S, Panwar N S. Dielectric properties of  $\text{Na}_{1-x}\text{K}_x\text{NbO}_3$  in orthorhombic phase. *Bull Mater Sci* 2003; 26[6] : 619 – 625.

37. Birol H, Damjanovic D, Setter N. Preparation and characterization of  $\text{Na}_{0.5}\text{K}_{0.5}\text{NbO}_3$  ceramics. *J. Eur Ceram Soc* 2006; 26 : 861 - 866.

38. Zhang B-P, Li J-F, Wang K, Zhang H. Compositional dependence of piezoelectric properties in  $\text{Na}_x\text{K}_{1-x}\text{NbO}_3$  lead-free ceramics prepared by spark plasma sintering. *J. Am Ceram Soc* 2006; 89[5] : 1605 - 1609.

39. Powder Diffraction File No. 32-0822, International Centre for Diffraction Data, Newton Square, PA, 2001.
40. Powder Diffraction File No. 32-0842, International Centre for Diffraction Data, Newton Square, PA, 2001.
41. Kim M-S, Lee D-S, Park E-C, Jeong S -J, Song J-S. Effect of  $\text{Na}_2\text{O}$  additions on the sinterability and piezoelectric properties of lead-free  $95(\text{Na}_{0.5}\text{K}_{0.5}\text{NbO}_3)-5\text{LiTaO}_3$  ceramics. *J. Eur Ceram Soc* 2007; in press.
42. Powder Diffraction File No. 34-0122, International Centre for Diffraction Data, Newton Square, PA, 2001.
43. Powder Diffraction File No. 80-0911, International Centre for Diffraction Data, Newton Square, PA, 2001.
44. Powder Diffraction File No. 80-0908, International Centre for Diffraction Data, Newton Square, PA, 2001.
45. Ahn Z S, Schulze W A. Conventionally sintered  $(\text{Na}_{0.5}\text{K}_{0.5}\text{NbO}_3)$  with barium additions. *J. Am Ceram Soc* 1987; 70[1] : C-18 – C-21.
46. Powder Diffraction File No. 48-0997, International Centre for Diffraction Data, Newton Square, PA, 2001.
47. Powder Diffraction File No. 84-2003, International Centre for Diffraction Data, Newton Square, PA, 2001.
48. Skidmore T A, Milne S J. Phase development during mixed-oxidized processing of a  $[(\text{Na}_{0.5}\text{K}_{0.5}\text{NbO}_3)]_{1-x} - [\text{LiTaO}_3]_x$  powder. *J Mater Res* 2007; in press.
49. Yang Z, Chang Y, Liu B, Wei L. *Mater Sci Eng A* 2006; 432 : 292-298.

## OUTPUT

จากโครงการวิจัยที่ได้รับทุนจาก สกอ.

## OUTPUT จากโครงการวิจัยที่ได้รับทุนจาก สกอ.

### 1. ผลงานที่ได้รับ/จัดส่งเพื่อตีพิมพ์ในวารสารวิชาการนานาชาติ จำนวนทั้งสิ้น 3 เรื่อง ได้แก่

#### 1.1 ผลงานวิจัยที่ได้ตีพิมพ์แล้ว 1 เรื่อง

- **Bomlai P**, Wichianrat P, Muensit S, Milne S J. Effects of calcination conditions and excess alkali carbonate on phase formation and particle morphology of  $(\text{Na}_{0.5}\text{K}_{0.5})\text{NbO}_3$  powders. *J Am Ceram Soc* 2007; 90[5] : 1650 - 1655. (ภาคผนวก ก)

#### 1.2 ผลงานวิจัยที่ได้จัดส่งเพื่อการตีพิมพ์ 2 เรื่อง

- **Bomlai P**, Wichianrat P, Muensit S, Milne S J. Effect of alkali carbonate excess on the properties of sodium potassium niobate ceramics. (manuscript submitted to special issue of Ceramic International) (ภาคผนวก ข)
- **Bomlai P**, Sukprasert S, Muensit S, Milne S J. Phase Development, Densification and Dielectric Properties of  $(0.95-x)\text{Na}_{0.5}\text{K}_{0.5}\text{NbO}_3 - 0.05\text{LiTaO}_3 - x\text{ LiSbO}_3$  Lead-free Piezoelectric Ceramics (manuscript submitted to Materials Research Bulletin) (ภาคผนวก ค)

### 2. ผลงานวิจัยที่ได้การตอบรับเพื่อตีพิมพ์ในวารสารวิชาการในประเทศ จำนวน 1 เรื่อง

- **Bomlai P**, Saengchote W, Muensit S, Milne S J. Effects of calcinations conditions and  $\text{K}_2\text{CO}_3$  content on phase and morphology evolution of  $(\text{Na}_{1-x}\text{K}_x)\text{NbO}_3$  powders. *Songklanakarin J Sci Technol* 2007; in press. (ภาคผนวก ง)

### 3. การนำผลงานวิจัยไปใช้ประโยชน์ คือ ประโยชน์เชิงวิชาการ

- สามารถสร้างองค์ความรู้ใหม่เกี่ยวกับการพัฒนาวัสดุชนิดใหม่เข้ามาใช้แทน PZT
- สามารถใช้งานวิจัยนี้เป็นส่วนหนึ่งในการพัฒนาการเรียนการสอนในหลักสูตรวัสดุศาสตร์ คณะวิทยาศาสตร์ มหาวิทยาลัยสงขลานครินทร์
- สามารถผลิตผลงานวิจัยเพื่อนำเสนอในงานประชุมเชิงวิชาการ และตีพิมพ์ในวารสารทางวิชาการทั้งในระดับชาติและนานาชาติได้
- สามารถผลิตนักวิจัยรุ่นใหม่ที่มีความรู้ความสามารถ และประสบการณ์ในการทำงานวิจัยที่มีคุณภาพต่อไปได้ในอนาคต

- สามารถสร้างเครื่องข่ายความร่วมมือในการทำงานวิจัยกับกลุ่มวิจัยที่เกี่ยวข้องทั้งจากภายในและนอกสถาบันได้

#### 4. การนำผลงานไปใช้ประโยชน์ด้านอื่นๆ

##### 4.1 การเข้าร่วมนำเสนอผลงานในงานประชุมเชิงวิชาการ

- ได้ไปเสนอผลงานวิจัยในการประชุม เรื่อง “The 5<sup>th</sup> Asian Meeting on Electroceramics (AMEC5)” ณ โรงแรมเช็นทรัล โซฟิเทล กรุงเทพ ในระหว่างวันที่ 10 – 14 ธันวาคม 2549  
**Bomlai P, Wichianrat P, Muensit S, Milne S J.** Effects of  $K_2CO_3$  and  $Na_2CO_3$  excess on the properties of sodium potassium niobate ceramics. The 5<sup>th</sup> Asian Meeting on Electroceramics (AMEC5) 10-14 Dec, 2006, 98, Bangkok, Thailand. (ภาคผนวก จ)
- ได้ไปเสนอผลงานวิจัยในการประชุม “นักวิจัยรุ่นใหม่..พน..เมธิวิจัยอาชญากรรม” ณ โรงแรมรีเจนท์ ชะอำ จังหวัดเพชรบุรี ในระหว่างวันที่ 12 – 14 ตุลาคม 2549  
**Bomlai P, Wichianrat P, Muensit S, Milne S J.** Effect of dopants on sintering behavior and properties of sodium potassium niobate ceramics. (ภาคผนวก ฉ)
- ได้ไปเสนอผลงานวิจัยในการประชุม “The 4<sup>th</sup> Thailand Materials Science and Technology Conference” ณ อุทยานวิทยาศาสตร์ประเทศไทย จังหวัดปทุมธานี ในระหว่างวันที่ 31 มีนาคม – 1 เมษายน 2549  
**Bomlai P.** Phase and Morphology Evolution of Sodium-potassium niobate Powder Synthesized by Solid-state Reaction, Proc. 4<sup>th</sup> Thailand Materials Science and Technology Conference, Bangkok, Thailand, Mar. 31-Apr. 1, 2006 : 52-54. (ภาคผนวก ฉ)

## Effect of Calcination Conditions and Excess Alkali Carbonate on the Phase Formation and Particle Morphology of $\text{Na}_{0.5}\text{K}_{0.5}\text{NbO}_3$ Powders

Pornsuda Bomlai<sup>†</sup> and Pattraporn Wichianrat

Materials Science Program, Prince of Songkla University, Songkla 90112 Thailand

Supasarute Muensit

Department of Physics, Prince of Songkla University, Songkla 90112 Thailand

Steven J. Milne

Institute for Materials Research, University of Leeds, Leeds LS2 9JT, U.K.

Sodium-potassium niobate [ $\text{Na}_{0.5}\text{K}_{0.5}\text{NbO}_3$ ] powders were prepared following the conventional mixed oxide method. An orthorhombic XRD pattern, consistent with single-phase  $\text{Na}_{0.5}\text{K}_{0.5}\text{NbO}_3$ , was obtained after calcination at  $900^\circ\text{C}$  for 6 h. Introducing 5 mol% excess  $\text{Na}_2\text{CO}_3$  and  $\text{K}_2\text{CO}_3$  into the starting mixture allowed milder calcination conditions to be used, for example  $800^\circ\text{C}$  for 2 h. Primary particles in 5 mol% excess samples were cuboid, with maximum sizes of  $\sim 2.5\text{ }\mu\text{m}$ . Equiaxed  $0.3\text{--}0.4\text{-}\mu\text{m}$  particles were formed for non-excess powders, and also for powders prepared with 1 and 3 mol% excess alkali carbonates. The results suggest liquid formation during calcination of the excess 5-mol% starting powders.

### I. Introduction

LEAD oxide-based ferroelectrics such as lead zirconate titanate  $[\text{Pb}(\text{Zr},\text{Ti})\text{O}_3$  or PZT] are widely used for piezoelectric actuators, sensors, and transducers due to their excellent piezoelectric properties.<sup>1–2</sup> Because of the detrimental effects of Pb on human health, it is important that Pb-free ferroelectric and piezoelectric materials are developed. The new environmentally acceptable and biocompatible materials should exhibit electrical properties comparable to those of Pb-based ferroelectrics, which have been developed over several decades.

Sodium-potassium niobate, [ $\text{Na}_{1-x}\text{K}_x\text{NbO}_3$  or NKN],-based ceramics are one of the most promising alternative systems to PZT.<sup>1,3</sup> The NKN solid solution system, between ferroelectric  $\text{KNbO}_3$  and antiferroelectric  $\text{NaNbO}_3$ , forms several morphotropic phase boundaries (MPB), one of which exists between two orthorhombic phases near the composition  $x = 0.5$ .<sup>1,4–5</sup> Although the piezoelectric properties of NKN solid solutions improve close to this MPB, they are still substantially inferior to PZT. However, it has been shown by Saito *et al.*<sup>6</sup> that Li and Ta ion substitution of the base  $\text{Na}_{0.5}\text{K}_{0.5}\text{NbO}_3$  composition, together with  $<001>$  grain orientation, results in piezoelectric  $d_{33}$  charge coefficients of  $\sim 400\text{ pC/N}$ . These values are very competitive with PZT. For randomly oriented  $(\text{K}_{0.5}\text{Na}_{0.5})_{1-x}\text{Li}_x(\text{Nb}_{1-y}\text{Ta}_y)\text{O}_3$  ceramics,  $d_{33}$  coefficients are  $\sim 200\text{--}300\text{ pC/N}$ .<sup>6–7</sup> Guo *et al.*<sup>3</sup> have studied the more simple

binary  $\text{Na}_{0.5}\text{K}_{0.5}\text{NbO}_3\text{--LiTaO}_3$  system, and for compositions at an MPB between tetragonal and orthorhombic phases,  $d_{33}$  values of  $\sim 200\text{ pC/N}$  have been reported for conventional, non-oriented, ceramic samples.

Specialist fabrication routes, including hot pressing and spark-plasma sintering, have been investigated in order to overcome the difficulties that have been encountered in fabricating high-density NKN-based ceramics.<sup>5,8–9</sup> However, there are also reports that high-density alkali niobate ceramics may be obtained by normal sintering methods, particularly if high-energy powder milling is used.<sup>9–12</sup> Whichever densification method is used, the most cost-effective means of producing a starting powder is by a mixed-oxide solid-state reaction route. For  $\text{Na}_{0.5}\text{K}_{0.5}\text{NbO}_3$ -based compositions, this normally involves calcination at  $\geq 800^\circ\text{C}$  for prolonged periods.<sup>1,3,5</sup> However, relatively little is known about the sequence of phase development, or particle formation, during powder calcination, even for the basic  $\text{Na}_{0.5}\text{K}_{0.5}\text{NbO}_3$  composition. The  $\text{Nb}_2\text{O}_5$  starting component is relatively refractory, with a melting point of  $1520^\circ\text{C}$ , whereas  $\text{Na}_2\text{CO}_3$  and  $\text{K}_2\text{CO}_3$  have much lower melting points,  $851^\circ$  and  $891^\circ\text{C}$ , respectively.<sup>13</sup> The alkali components therefore become volatile at moderate calcination temperatures, and this combination of properties in the starting reagents makes it potentially difficult to prepare chemically homogeneous, single-phase alkali niobate powders by the mixed-oxide route. Variability between starting powders may in part be responsible for some of the reported discrepancies in the densification characteristics of NKN-based ceramics.

The present communication investigates phase development in  $\text{Na}_{0.5}\text{K}_{0.5}\text{NbO}_3$  powders as a function of calcination conditions. The effects of introducing excess alkali carbonates into the starting mixture, in order to compensate for probable alkali oxide losses during calcination, are considered. Particle size and morphology are also evaluated for different calcination temperatures and dwell times.

### II. Experimental Procedure

Samples were prepared by the conventional mixed-oxide process using  $\text{K}_2\text{CO}_3$  (Sigma-Aldrich, St. Louis, MO,  $\geq 99.0\%$  purity),  $\text{Na}_2\text{CO}_3$ , and  $\text{Nb}_2\text{O}_5$  (Sigma-Aldrich, 99.9+% purity), for which SEM micrographs are shown in Fig. 1. The two carbonate powders are moisture sensitive; thermogravimetric analysis indicates that dehydration is completed at  $\sim 200^\circ\text{C}$ , and therefore to avoid compositional errors when weighing out the  $\text{Na}_{0.5}\text{K}_{0.5}\text{NbO}_3$  precursor mixture, the starting reagents were dried in an oven for 24 h before use. Dried powders were

D. Payne—contributing editor

Manuscript No. 22306. Received September 29, 2006; approved January 22, 2007.  
 This work was supported by Thailand Research Fund (TRF) and Commission on Higher Education.  
<sup>†</sup>Author to whom correspondence should be addressed. e-mail: ppornsuda@yahoo.com

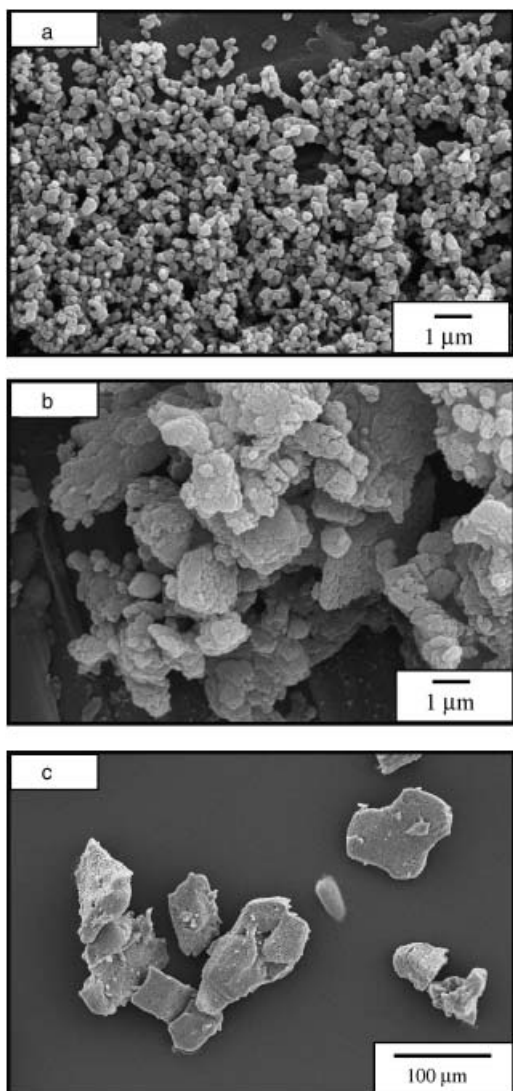


**Fig. 1.** Scanning electron microscopy micrographs of the starting powders: (a)  $\text{Nb}_2\text{O}_5$ , (b)  $\text{Na}_2\text{CO}_3$ , (c)  $\text{K}_2\text{CO}_3$ . The carbonates are hydrated phases.

allowed to cool to room temperature under reduced pressure in a dessicator, and all powders were stored in the dessicator until immediately before weighing in the correct proportions. The starting materials, 30 g, were transferred to a 100-mm diameter cylindrical plastic jar and partially filled with 10-mm diameter alumina grinding balls occupying ~40% of the total volume of the container. Sufficient ethanol was added to cover the powder/media and bring the final volume to ~50% of the jar. Ball milling was carried out for 24 h, followed by drying at 120°C for 24 h, before grinding with an alumina mortar and pestle. The mixtures were calcined in alumina crucibles, with loosely fitting lids, at temperatures ranging from 600° to 950°C, with dwell times of 2, 6, and 10 h. Powders containing excess  $\text{Na}_2\text{CO}_3$  and  $\text{K}_2\text{CO}_3$ , at levels of 1, 3, and 5 mol% were prepared using similar procedures. This type of approach is often used for PZT powders by adding excess  $\text{PbO}$  to compensate for the volatility of  $\text{PbO}$ . In the present work, powder samples were made with an equimolar ratio of  $\text{Na}_2\text{CO}_3$  and  $\text{K}_2\text{CO}_3$ .

Calced powders were examined at room temperature using X-ray powder diffraction (XRD; Philips X' Pert MPD, Eindhoven, the Netherlands; Ni-filtered  $\text{CuK}$  radiation) to identify the phase(s) formed. Powders were imaged directly, using scanning electron microscopy (SEM; JEOL, Tokyo, Japan, JSM-5800LV) in order to gain information on the particle size and morphology for the various calcination conditions, and starting alkali carbonate contents. For ceramic fabrication, powders cal-

cined at 900°C for 2 h, or in the case of the 5 mol% excess powder 800°C for 2 h, were pressed at 100 MPa into 1.5-cm diameter disks and sintered in air at 1140°C for 2 h in closed crucibles. Sintered pellet densities were obtained by measuring their dimensions and mass.

### III. Results and Discussion

The XRD patterns of batches of powder, prepared from stoichiometric starting mixtures, calcined at different temperatures in the range 600°–950°C for 2 h are shown in Fig. 2(a). Broad peaks near the expected positions of the desired sodium potassium niobate phase were present in the sample calcined at 600°C for 2 h.<sup>3,14,15</sup> However, closely spaced peaks characteristic of the orthorhombic  $\text{Na}_{0.5}\text{K}_{0.5}\text{NbO}_3$  pattern<sup>3,14,15</sup> could not be distinguished until much higher calcination temperatures, 900° and 950°C. In samples calcined at temperatures  $\leq 900^\circ\text{C}$  for 2 h, a low-intensity extra peak ( $I/I_0 \sim 4\%$ ) was present at 28.4°20, Fig. 2(b), which is attributed to unreacted  $\text{Nb}_2\text{O}_5$ , the major component of the starting mixture.<sup>16</sup> There was no conclusive evidence of any intermediate binary alkali niobates at these temperatures.

Overall, these observations suggest that the majority of the starting  $\text{K}_2\text{CO}_3$ ,  $\text{Na}_2\text{CO}_3$ , and  $\text{Nb}_2\text{O}_5$  had reacted to form sodium potassium niobate at relatively low calcination temperatures. However, broadening of the XRD peaks, and the progressive peak sharpening as the calcination temperature was increased, suggest that the product at 600°–850°C was not a chemically homogeneous solid solution phase. Any spatial variations in the Na and K ratios due to imperfect mixing and incomplete reaction would produce a series of NKN solid solution compositions with differing values of  $x$ , in different regions of the sample. Because of the small shifts in d spacings with changing composition reported for intermediate values of  $x$ ,<sup>4,15</sup> an overlap of XRD peaks from compositionally inhomogeneous regions would occur, and result in single broad peaks, as shown in Fig. 2 for temperatures  $\leq 850^\circ\text{C}$ . As calcination temperatures increase to 900° and 950°C, the NKN solid solution becomes more homogeneous, XRD peaks become narrower, and a pattern similar to that expected for orthorhombic  $\text{Na}_{0.5}\text{K}_{0.5}\text{NbO}_3$  is produced, in which closely spaced peaks such as the 101 and 001 peaks at  $\sim 22^\circ\text{20}$  can be resolved.

The effect of increasing the dwell time from 2 to 6 and 10 h was investigated for powders calcined at 900°C. The peak indicating unreacted  $\text{Nb}_2\text{O}_5$  disappeared when the calcination period was increased to 6 h, but no other changes were observed in either the 6- or 10-h samples.

An excess of 5 mol%  $\text{Na}_2\text{CO}_3$  and  $\text{K}_2\text{CO}_3$  was found to have a significant effect on phase development. Peak splitting showing well-crystallized NKN became apparent after calcination at 800°C, as opposed to 900°C for the other powders (Fig. 3). In addition, evidence of unreacted starting material disappeared at a calcination temperature of 700°C, which is 200°C lower than for standard, non-excess powders. Reducing the level of additive to 3 mol% produced XRD patterns similar to those of the non-excess powders, but the calcination period at 900°C required to eliminate second phase  $\text{Nb}_2\text{O}_5$  was reduced from 6 to 2 h (Fig. 4). Estimated lattice parameters were  $a = 5.59 \text{ \AA}$ ,  $b = 15.73 \text{ \AA}$ , and  $c = 5.67 \text{ \AA}$  for all sample types; these are similar to the values reported in the literature.<sup>17</sup>

The dependence of particle size and morphology on calcination temperature, dwell time, and the level of excess alkali carbonate is shown in Fig. 5; particle size ranges observed in SEM images are summarized in Table I. For standard, non-excess powders, calcination at 700°C for 2 h resulted in equiaxed particles, with estimated maximum primary particle sizes of  $\sim 0.15 \mu\text{m}$ . The maximum size increased to  $\sim 0.2 \mu\text{m}$  at 800°C and to  $\sim 0.3 \mu\text{m}$  at 900°C (Fig. 5). Increasing the dwell time at 900°C from 2 to 10 h resulted in maximum sizes of  $\sim 0.4 \mu\text{m}$ .

Particle properties of 1 and 3 mol% powders were similar to the non-excess powders. However, the samples made with

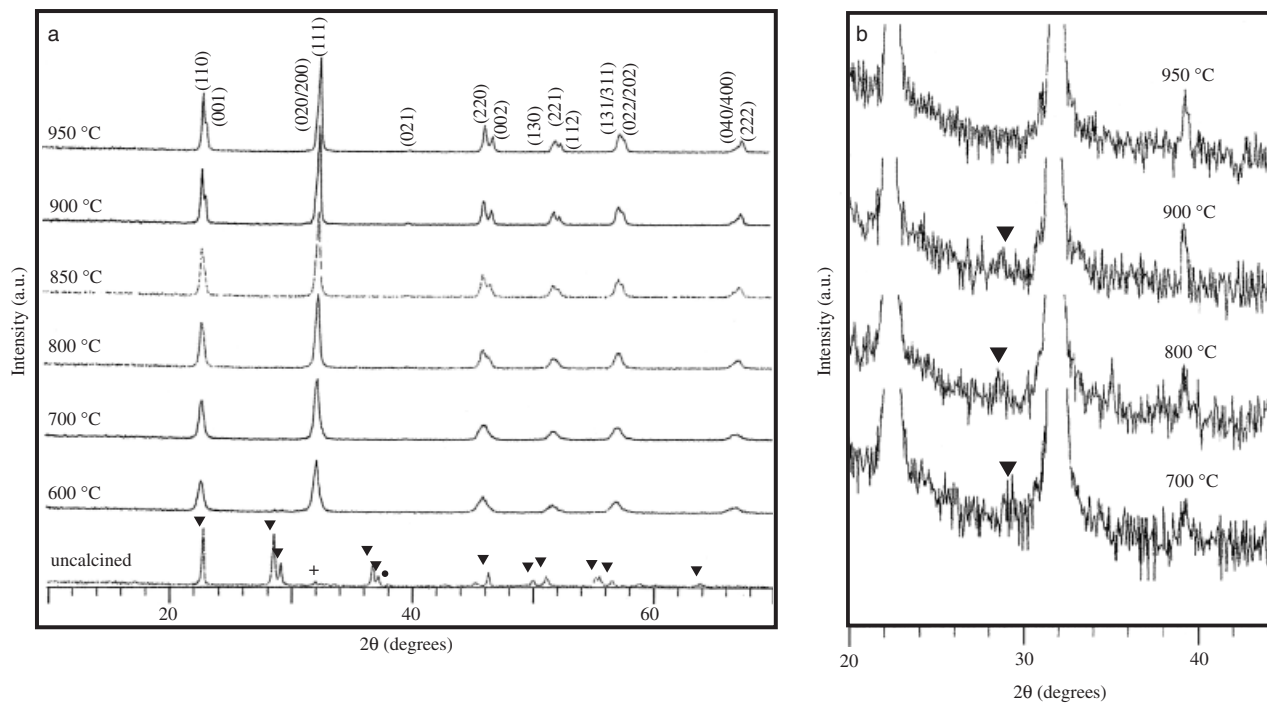


**Fig. 2.** (a) X-ray diffraction (XRD) patterns of  $\text{Na}_{1-x}\text{K}_x\text{NbO}_3$  (NKN) powders calcined at various temperatures for 2 h; the pre-calcined mixture is also shown ( $\blacktriangledown$ ,  $\text{Nb}_2\text{O}_5$ ; +,  $\text{K}_2\text{CO}_3$ ; ●,  $\text{Na}_2\text{CO}_3$ ). The orthorhombic pattern is indexed according to JCPDS data file 32-0822.<sup>21</sup> (b) The expanded XRD patterns of NKN powders calcined at various temperatures for 2 h ( $\blacktriangledown$ ,  $\text{Nb}_2\text{O}_5$ ).<sup>16</sup>

5-mol% excess alkali carbonate showed a major difference in particle morphology and size (Figs. 5(d)–(f)). Between 700° and 800°C, the shape changed from approximately equiaxed to cuboid, and the maximum particle size increased to  $\sim 1 \mu\text{m}$  (Fig. 5(d) and (e)). Increasing the calcination temperature to 900°C resulted in particles up to  $\sim 2.5 \mu\text{m}$  in edge length (Fig. 5(f)). Intergrowth of the cuboid particles was evident, par-

ticularly at the highest calcination temperature, resulting in agglomerates with strong interparticle necking (Fig. 5(f)).

The characteristic cuboid particle morphology in the 5 mol% excess alkali powders indicates that the additive leads to a very different  $\text{Na}_{0.5}\text{K}_{0.5}\text{NbO}_3$  particle formation mechanism. The increased size and the cuboid shape of the particles are indicative of secondary crystallization (exaggerated particle growth). In

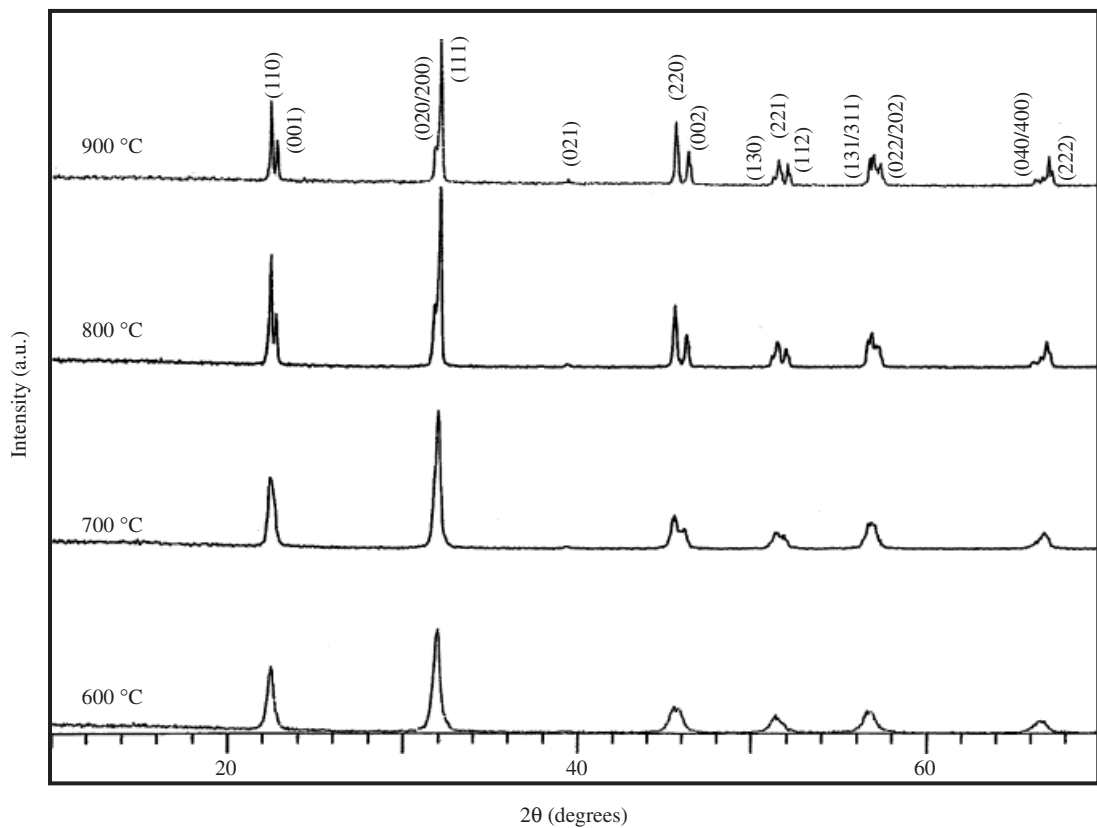


**Fig. 3.** X-ray diffraction patterns of  $\text{Na}_{1-x}\text{K}_x\text{NbO}_3$  powders with 5 mol% excess of  $\text{K}_2\text{CO}_3$  and  $\text{Na}_2\text{CO}_3$  calcined at various temperatures for 2 h.

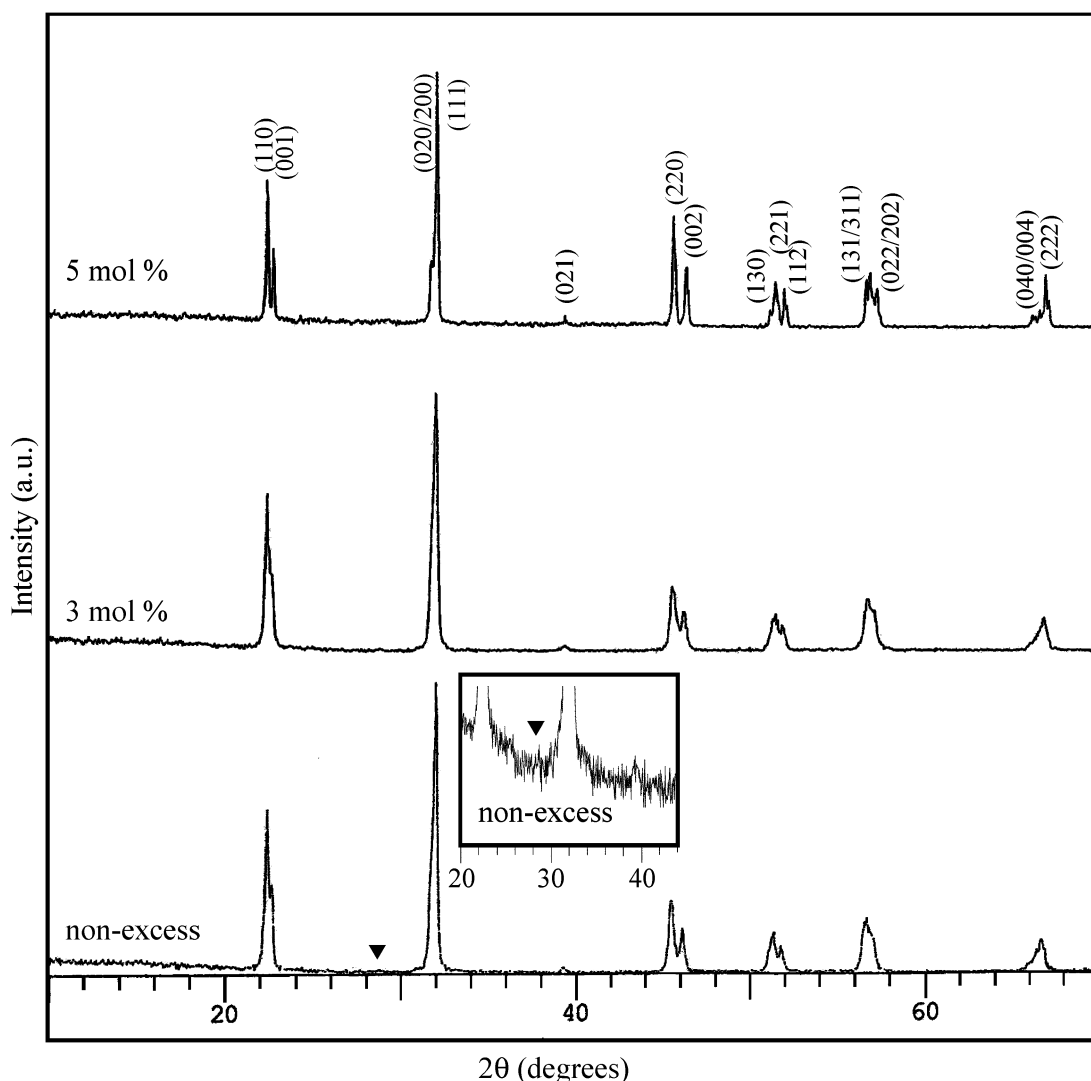


Fig. 4. X-ray diffraction patterns of  $\text{Na}_{1-x}\text{K}_x\text{NbO}_3$  powders with various amounts of  $\text{K}_2\text{CO}_3$  and  $\text{Na}_2\text{CO}_3$  excess calcined at  $900^\circ\text{C}$  for 2 h. (▼,  $\text{Nb}_2\text{O}_5$  peak, which appears only in the non-excess sample under these conditions (see inset diagram).

this type of particle growth process, large particles grow by consuming small particles; evidence of this was found in partially formed cuboid particles in the  $800^\circ\text{C}$  sample. The regular particle morphology results from the preferential growth of low surface energy planes. A liquid phase is often associated with the related mechanism of secondary crystallization during high-temperature sintering of perovskite ceramics, leading to large angular grains. The present results for particle growth during the calcination of  $\text{Na}_{0.5}\text{K}_{0.5}\text{NbO}_3$  powders infer the presence of a particle–liquid interface in the 5-mol% excess carbonate samples at  $\geq 800^\circ\text{C}$ , and this was responsible for the change in the particle growth mechanism.

A published detailed phase diagram of the ternary  $\text{Na}_2\text{CO}_3$ – $\text{K}_2\text{CO}_3$ – $\text{Nb}_2\text{O}_5$  system is not available to help interpret the relationships between phase content, particle properties, and starting alkali carbonate composition. Phase equilibria for the binary join,  $\text{NaNbO}_3$ – $\text{KNbO}_3$  indicate  $\text{Na}_{0.5}\text{K}_{0.5}\text{NbO}_3$  to undergo partial melting at  $\sim 1100^\circ\text{C}$ .<sup>2</sup> The present results could point to much lower melting temperatures for  $\text{Na}_2\text{CO}_3$ – $\text{K}_2\text{CO}_3$ – $\text{Nb}_2\text{O}_5$  ternary mixtures on the alkali-rich side of the  $\text{NaNbO}_3$ – $\text{KNbO}_3$  join, for compositions equivalent to  $\sim 5$ -mol% excess of equimolar  $\text{Na}_2\text{CO}_3$  and  $\text{K}_2\text{CO}_3$ . Alternatively, a liquid could form under non-equilibrium conditions due to melting of the excess alkali carbonates at an early stage of the calcination reaction. Pure sodium and potassium carbonates melt at  $851^\circ$  and  $891^\circ\text{C}$ , respectively,<sup>13</sup> but these temperatures are higher than the present implied liquid formation temperature of between  $700^\circ$  and  $800^\circ\text{C}$ . However, reference to a phase diagram of the

$\text{Na}_2\text{CO}_3$ – $\text{K}_2\text{CO}_3$  system indicates that under equilibrium conditions, melting temperatures of mixtures of the two carbonates decline to a minimum of  $\sim 710^\circ\text{C}$  at a composition  $\sim 55$ -mol%  $\text{Na}_2\text{CO}_3$ .<sup>18</sup> This composition is close to that of the starting excess used here (50 mol%).

Hence, melting of the equimolar mixture of residual excess alkali carbonates could provide a straightforward explanation of liquid formation in the excess carbonate powders calcined at  $\geq 800^\circ\text{C}$ . It is assumed that eventually all of the excess alkali oxides, over and above the level required to maintain the stoichiometry of the NKN product, will evaporate during the latter stages of calcination, and the composition equilibrates to  $\text{Na}_{0.5}\text{K}_{0.5}\text{NbO}_3$ . In the 5-mol% sample, volatilization of the excess portion is presumed to be incomplete, creating conditions where liquid formation occurs. In the case of the 1- and 3-mol% samples, there is insufficient excess carbonate remaining to cause any major changes to reaction conditions.

The cuboid particle shape is similar to the form we have observed for particles of the orthorhombic  $\text{NaNbO}_3$  end member made via a hydrothermal synthesis method, involving secondary crystallization.<sup>19</sup> An increased rate of mass transport, due to the presence of a transient liquid, would also allow a highly homogeneous solid solution to be produced under milder calcination conditions, as found from the XRD results.

The 5-mol% powders calcined at  $900^\circ\text{C}$  showed the sharpest XRD peaks of any of the samples investigated (Figs. 2–4). The slightly more diffuse XRD peaks in the patterns of the other powders for the maximum calcination temperatures probably

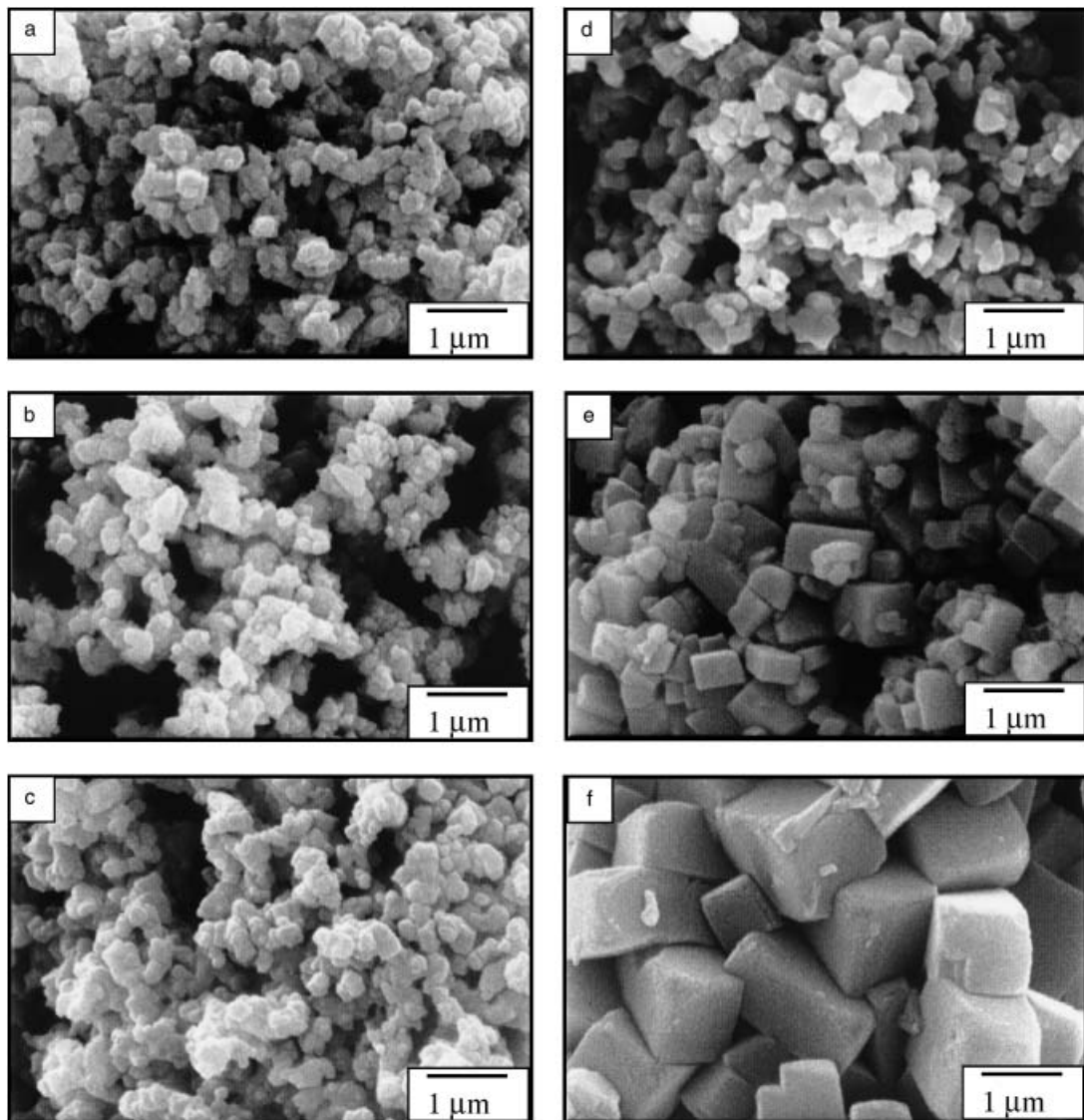


**Fig. 5.** Scanning electron microscopy micrographs of the calcined  $\text{Na}_{1-x}\text{K}_x\text{NbO}_3$  powders: non-excess powders (a) 700°C, (b) 800°C, (c) 900°C; and 5-mol% excess  $\text{Na}_2\text{CO}_3$  and  $\text{K}_2\text{CO}_3$  powders, (d) 700°C, (e) 800°C, and (f) 900°C.

reflect some continuing distribution in Na/K ratios, but on a much reduced scale compared with lower temperature samples ( $\leq 850^\circ\text{C}$ ). There may also be some contribution to peak-broadening effects from the much smaller crystallite sizes (Table I).<sup>20</sup>

In terms of preparing suitable  $\text{Na}_{0.5}\text{K}_{0.5}\text{NbO}_3$  powders for ceramic fabrication, the present study indicates that adding 5-mol% excess  $\text{Na}_2\text{CO}_3$  and  $\text{K}_2\text{CO}_3$  enables lower calcination temperatures and shorter times to be used. Normally, this would be beneficial for ceramic fabrication, as smaller particle sizes and weaker agglomerates would be expected. However, the change in the particle formation mechanism leads to much larger particles, and strong inter-particle necking giving a less sinter-active powder. Preliminary ceramic fabrication trials support this view. Table II illustrates the densities of sintered pellets prepared from the powders containing 0–5 mol% of starting excess carbonates; each powder was calcined at the minimum temperature to produce an orthorhombic XRD pattern. The non-excess samples reached a density of  $3.91 \text{ g/cm}^3$ , increasing slightly for 1-mol% additions, and reaching a maximum value of  $4.14 \text{ g/cm}^3$  for 3-mol% excess, before declining to  $\sim 3.83 \text{ g/cm}^3$  for the 5-mol% excess carbonate starting powder. These values represent an increase from  $\sim 86\%$  to a maximum of  $\sim 91\%$  theoretical density for the 3-mol% excess sample (assuming a theoretical value<sup>10</sup> of  $4.51 \text{ g/cm}^3$ ). The decrease in density on moving from 3 to 5 mol % of the additive is attributed to the larger particles in the latter powders. The lower density of the non-excess and 1% excess

pellets may be associated with uncompensated alkali oxide losses from the NKN product phase. The limiting sintered geometric density for the optimum level of excess carbonates is around 3% lower than the Archimedes density values reported for NKN ceramics made from (non-excess) powders prepared using planetary milling.<sup>10</sup> In part, this may be due to differences in measurement techniques, as at these porosity levels, geometric densities are often lower than the corresponding values

**Table I. Particle Size Ranges of  $(\text{Na}_{0.5}\text{K}_{0.5})\text{NbO}_3$  Powders Calcined under Various Conditions**

Calcination conditions			
Temperature (°C)	Dwell time (h)	Excess of $\text{K}_2\text{CO}_3$ and $\text{Na}_2\text{CO}_3$ (mol %)	Particle size range (μm)
700	2	0	0.1–0.15
800	2	0	0.10–0.2
900	2	0	0.15–0.30
900	10	0	0.30–0.40
900	2	3	0.25–0.50
700	2	5	0.18–0.22
800	2	5	0.30–1.0
900	2	5	1.0–2.5

**Table II. Density of Sintered Pellets Made from Powders with Different Levels of Excess  $\text{Na}_2\text{CO}_3$  and  $\text{K}_2\text{CO}_3$  in the Starting Mixtures**

Excess of $\text{K}_2\text{CO}_3$ and $\text{Na}_2\text{CO}_3$ (mol%)	Measured density (g/cm <sup>3</sup> )	Relative density (%)
0	3.91	86
1	3.99	88
3	4.14	91
5	3.83	84

measured by water displacement. The literature suggests that significantly higher densities than 91% could be achieved for the NKN-3-mol% excess powders by replacing ball milling with high-energy attrition milling.<sup>7,10,12</sup>

#### IV. Conclusions

Powders of  $\text{Na}_{0.5}\text{K}_{0.5}\text{NbO}_3$  were prepared by a mixed-oxide route under various calcination conditions. Evidence gained from XRD revealed that an orthorhombic single-phase product with particle sizes  $\leq 0.4 \mu\text{m}$  could be obtained by calcination at 900°C for 6 h. Adding 5-mol% excess of  $\text{Na}_2\text{CO}_3$  and  $\text{K}_2\text{CO}_3$  allowed a well-crystallized  $\text{Na}_{0.5}\text{K}_{0.5}\text{NbO}_3$  phase to be produced under milder calcination conditions, for example 800°C for 2 h. A change in particle shape to a cuboid form, coupled with an increase in particle size, may be due to the formation of a liquid phase during calcination of 5-mol% excess alkali carbonate powders. The maximum-sintered density was achieved for 3 mol% of the combined additive; particles in these calcined powders were similar to those of non-excess samples.

#### Acknowledgment

Thanks are due to Tom Skidmore for useful comments.

#### References

- Y. Guo, K.-I. Kakimoto, and H. Ohsato, "Dielectric and Piezoelectric Properties of Lead-Free  $(\text{Na}_{0.5}\text{K}_{0.5})\text{NbO}_3$ – $\text{SrTiO}_3$  Ceramics," *Solid State Commun.*, **129** [5] 279–84 (2004).
- B. Jaffe, W. R. Cook, and H. Jaffe, *Piezoelectric Ceramics*. Academic Press, New York, 1971.
- Y. Guo, K.-I. Kakimoto, and H. Ohsato, " $(\text{Na}_{0.5}\text{K}_{0.5})\text{NbO}_3$ – $\text{LiTaO}_3$  Lead-Free Piezoelectric Ceramics," *Mater. Lett.*, **59**, 241–4 (2005).
- G. Shirane, R. Newnham, and R. Pepinsky, "Dielectric Properties and Phase Transition of  $\text{NaNbO}_3$  and  $(\text{Na}, \text{K})\text{NbO}_3$ ," *Phys. Rev.*, **96** [3] 581–8 (1954).
- R. Wang, R. Xie, T. Sekiya, and Y. Shimojo, "Fabrication and Characterization of Potassium–Sodium Niobate Piezoelectric Ceramics by Spark-Plasma Sintering Method," *Mater. Res. Bull.*, **39**, 1709–15 (2004).
- Y. Saito, H. Takao, T. Tani, T. Nonoyama, K. Takatori, T. Homma, T. Nagaya, and M. Nakamura, "Lead-Free Piezoceramics," *Nature*, **432**, 84–7 (2004).
- Y. Saito and H. Takao, "High Performance Lead-Free Piezoelectric Ceramics in the  $(\text{K}, \text{Na})\text{NbO}_3$ – $\text{LiTaO}_3$  Solid Solution System," *Ferroelectrics*, **338**, 17–32 (2006).
- R. E. Jaeger and L. Egretton, "Hot Pressing of Potassium–Sodium Niobates," *J. Am. Ceram. Soc.*, **45** [5] 209–13 (1962).
- J.-F. Li, K. Wang, B.-P. Zhang, and L.-M. Zhang, "Ferroelectric and Piezoelectric Properties of Fine-Grained  $\text{Na}_{0.5}\text{K}_{0.5}\text{NbO}_3$  Lead-Free Piezoelectric Ceramics Prepared by Spark Plasma Sintering," *J. Am. Ceram. Soc.*, **89** [2] 706–9 (2006).
- R. Zuo, J. Rödel, R. Chen, and L. Li, "Sintering and Electrical Properties of Lead-Free  $\text{Na}_{0.5}\text{K}_{0.5}\text{NbO}_3$  Piezoelectric Ceramics," *J. Am. Ceram. Soc.*, **89** [6] 2010–5 (2006).
- H. Birol, D. Damjanovic, and N. Setter, "Preparation and Characterization of  $\text{KNbO}_3$  Ceramics," *J. Am. Ceram. Soc.*, **88** [7] 1754–9 (2005).
- E. Hollenstein, M. Davis, D. Damjanovic, and N. Setter, "Piezoelectric Properties of Li- and Ta-Modified  $(\text{K}_{0.5}\text{Na}_{0.5})\text{NbO}_3$  Ceramics," *Appl. Phys. Lett.*, **87**, 1–3 (2005).
- D. R. Lide, *Handbook of Chemistry and Physics*, 74th edition, CRC Press, Boca Raton, FL, 1993.
- H. Birol, D. Damjanovic, and N. Setter, "Preparation and Characterization of  $(\text{K}_{0.5}\text{Na}_{0.5})\text{NbO}_3$  Ceramics," *J. Eur. Ceram. Soc.*, **26**, 861–6 (2005).
- B.-P. Zhang, J.-F. Li, K. Wang, and H. Zhang, "Compositional Dependence of Piezoelectric Properties in  $\text{Na}_x\text{K}_{1-x}\text{NbO}_3$  Lead-Free Ceramics Prepared by Spark Plasma Sintering," *J. Am. Ceram. Soc.*, **89** [5] 1605–9 (2006).
- Powder Diffraction File No. 30–0873, International Centre for Diffraction Data, Newton Square, PA, 2001.
- V. Lingwal, B. S. Semwal, and N. S. Panwar, "Dielectric Properties of  $\text{Na}_{1-x}\text{K}_x\text{NbO}_3$  in Orthorhombic Phase," *Bull. Mater. Sci.*, **26** [6] 619–25 (2003).
- E. M. Levin, C. R. Robbins, and H. F. McMurdie, *Phase Diagrams for Ceramists*. The American Ceramic Society, Columbus, 1964.
- J. He, T. Skidmore, and S. J. Milne, "Fabrication and Characterization of Lead-Free Piezoelectric Ceramics," unpublished work.
- B. D. Cullity and S. R. Stock, *Elements of X-ray Diffraction*. Prentice Hall, Upper Saddle River, NJ, 2001.
- Powder Diffraction File No. 32–0822, International Centre for Diffraction Data, Newton Square, PA, 2001. □

# **Effect of alkali carbonates excess on the properties of sodium potassium niobates ceramics**

**Pornsuda Bomlai<sup>a,\*</sup>, Pattraporn Wichianrat<sup>a</sup>, Supasarote Muensit<sup>b</sup> and Steven J. Milne<sup>c</sup>**

<sup>a</sup>*Materials Science Program, and <sup>b</sup>Department of Physics, Faculty of Science,*

*Prince of Songkla University, Songkla 90112 Thailand*

<sup>c</sup>*Institute for Materials Research, University of Leeds, Leeds LS2 9JT, United Kingdom.*

## **Abstract**

Nowadays, lead-free materials have been urgently demanded from the viewpoint of environmental protection. One of the promising candidates to replace the lead containing materials is sodium potassium niobate. In present work, sodium-potassium niobate ((Na<sub>0.5</sub>K<sub>0.5</sub>)NbO<sub>3</sub>; NKN) ceramics with excess of alkali carbonate starting powders (0, 0.01, 0.03 and 0.05 mol) were prepared by solid – state reaction. The results showed that the amount of K<sub>2</sub>CO<sub>3</sub> and Na<sub>2</sub>CO<sub>3</sub> excess affected significantly to sintering temperature, bulk density, microstructure and dielectric property. Whereas, the XRD result showed the orthorhombic phase and there was no secondary phase formed in all samples. The highest dielectric constant value was found to be 1707 for sample with excess of 0.01 mol when sintered at 1100 °C. This is believed that the uniform microstructure and smaller in grain size were obtained.

**Keywords:** Powders: solid state reaction, Dielectric properties, Niobates, Microstructure- final

\*Corresponding author: e-mail address: ppornsuda@yahoo.com (P. Bomlai),

Tel: +6674 288 250, Fax : + 6674 218 701

## 1. Introduction

Lead oxide based ferroelectrics such as lead zirconate titanate [Pb(Zr,Ti)O<sub>3</sub> or PZT] are widely used for piezoelectric actuators, sensors and transducers due to their excellent piezoelectric properties [1-2]. Because of the detrimental effects of lead on human health, and because of European Union legislation it is important that Pb-free ferroelectric and piezoelectric materials are developed. The new environmentally acceptable and biocompatible materials should exhibit electrical properties comparable to those of Pb-based ferroelectrics, which have been developed over several decades.

Sodium-potassium niobate, [Na<sub>1-x</sub>K<sub>x</sub>NbO<sub>3</sub> or NKN], based ceramics are one of the most promising alternative systems to PZT [1, 3]. The Na<sub>1-x</sub>K<sub>x</sub>NbO<sub>3</sub> solid solution system, between ferroelectric KNbO<sub>3</sub> and antiferroelectric NaNbO<sub>3</sub>, forms several morphotropic phase boundaries (MPB), one of which exists between two orthorhombic phases near the composition x = 0.5 [1,4-5]. Although the piezoelectric properties of NKN solid solutions improve close to this MPB, they are still substantially inferior to PZT. However it has been shown by Saito et al. that Li and Ta ion substitution of the base Na<sub>0.5</sub>K<sub>0.5</sub>NbO<sub>3</sub> composition, together with <001> grain-orientation, results in piezoelectric d<sub>33</sub> charge coefficients of ~ 400 pC/N. These values are very competitive with PZT [6]. For randomly oriented (K<sub>0.5</sub>Na<sub>0.5</sub>)<sub>1-x</sub>Li<sub>x</sub>(Nb<sub>1-y</sub>Ta<sub>y</sub>)O<sub>3</sub> ceramics, d<sub>33</sub> coefficients are ~ 200-250 pC/N [6-7]. Guo et al. have studied the more simple binary Na<sub>0.5</sub>K<sub>0.5</sub>NbO<sub>3</sub> – LiTaO<sub>3</sub> system, and for compositions at a MPB between tetragonal and orthorhombic phases, d<sub>33</sub> values of ~ 200 pC/N are reported for conventional, non-oriented, ceramic samples [3].

Specialist fabrication routes, including hot-pressing and spark-plasma sintering, have been investigated in-order to overcome difficulties which have been encountered in fabricating high density NKN-based ceramics [5, 8-9]. However there are also reports that high density alkali niobate ceramics may be obtained by normal sintering methods, particularly if efficient milling is used prior to compaction [9, 10-12]. Whichever densification method is employed, the most cost-effective means of producing a starting powder is by a mixed-oxide solid state reaction route. The  $\text{Nb}_2\text{O}_5$  starting component is relatively refractory, with a melting point of 1520 °C, whereas  $\text{Na}_2\text{CO}_3$  and  $\text{K}_2\text{CO}_3$  have much lower melting points, 851 °C and 891 °C, respectively [13]. The alkali components therefore become volatile at moderate calcination or sintering temperatures, and this combination of properties in the starting reagents makes it potentially difficult to prepare chemically homogeneous, single-phase alkali niobate powders by the mixed-oxide route. Variability in the starting powders may in-part be responsible for some of the reported discrepancies in the densification characteristics of NKN- based ceramics.

The present work, the effects of introducing excess alkali carbonates to the starting mixture as a function of sintering conditions, in order to compensate for probable alkali oxide losses during calcination or sintering on phase development and the properties in  $\text{Na}_{0.5}\text{K}_{0.5}\text{NbO}_3$  ceramics were investigated.

## 2. Experimental procedure

Samples containing excess of  $\text{Na}_2\text{CO}_3$  and  $\text{K}_2\text{CO}_3$ , at levels of 0, 1, 3 and 5 mol% were prepared by the conventional mixed-oxide process using  $\text{K}_2\text{CO}_3$  (Aldrich Chemical Company, Inc.,  $\geq 99.0\%$  purity),  $\text{Na}_2\text{CO}_3$  and  $\text{Nb}_2\text{O}_5$  (Aldrich Chemical

Company, Inc., 99.9+% purity). This type of approach is often used for PZT powders by adding excess PbO to compensate for the volatility of PbO (losses during subsequent sintering can be addressed by using an ‘atmosphere’ powder). In the present work, powder samples were made with an equimolar ratio of  $\text{Na}_2\text{CO}_3$  and  $\text{K}_2\text{CO}_3$ . These two carbonate powders are moisture-sensitive; thermogravimetric analysis indicates that dehydration is completed at  $\sim 200$  °C, therefore to avoid compositional errors when weighing out the  $\text{Na}_{0.5}\text{K}_{0.5}\text{NbO}_3$  precursor mixture, the starting reagents were dehydrated in an oven for 24 h prior to use. Dried powders were allowed to cool to room temperature under reduced pressure in a dessicator, and all powders were stored in the dessicator until immediately prior to weighing in the correct proportions. The mixed starting materials were transferred to a plastic jar containing 10 mm-diameter alumina grinding balls. Ball-milling was carried out for 24 h using ethanol as the liquid medium; this was followed by drying at 120 °C for 24 h, prior to grinding with an alumina mortar and pestle. The mixtures were calcined in alumina crucibles at 900 °C, exempt sample with 5 mol% excess was calcined at 800 °C, for 2 h with loosely fitting lids. The calcined powder was ball-milled in ethanol again for 24 h. After drying, it was mixed thoroughly with a PVA binder solution and uniaxially pressed at 100 MPa into disk samples with a diameter of 15 mm. The disk samples were then sintered in air at temperature ranging from 1075 - 1160 °C for 2 h, using heating and cooling rates of 5 °C/min.

Phase formation in the polished surfaces of sintered samples was examined at room temperature using X-ray powder diffraction (XRD; Philips X’Pert MPD, Ni-filtered  $\text{CuK}_\alpha$  radiation). The geometric density of samples was calculated by mass and volume. The microstructures of the as-sintered surfaces of the samples were imaged

directly, using scanning electron microscopy (SEM; Jeol : JSM-5800LV). To investigate dielectric property, capacitance and loss tangents ( $\tan \delta$ ) of sample with silver paste electrode was measured at room temperature using a LCR meter (HP 4263B) on the basis of frequency, and the relative permittivity ( $\epsilon_r$ ) was then calculated.

### 3. Results and Discussion

The XRD patterns of samples with different alkali carbonate starting powders sintered at 1140 °C for 2 h are shown in Fig 1. The diffracted peaks are identified to perovskite phase with orthorhombic structure, formed without secondary phase in all samples. An excess of 5 mol%  $\text{Na}_2\text{CO}_3$  and  $\text{K}_2\text{CO}_3$  was found to have a significant effect on phase development, but 1-3 mol % produced similar results to the non-excess samples. This is confirmed that the increase of diffraction peak intensities was obtained. The addition of excess alkali carbonates had no measurable effect on d-spacings, with estimated lattice parameters:  $a = 5.59$ ,  $b = 15.73$  and  $c = 5.67$  Å for all sample-types. These values are similar to those reported in the literature [14].

The density of samples as a function of amount of alkali carbonate and sintering temperature is shown in Fig. 2. The density of non-excess sample decreased significantly with increasing of sintering temperature. This is due to the loss of alkali oxide during sintering. After introducing excess alkali carbonates, the maximum density was reach to 4.14 g/cm<sup>3</sup> for the sample containing 0.03 mol% of alkali carbonate powders at sintering temperature of 1140 °C. The density values represent an increase from ~ 89 % to 92 % theoretical density (assuming a theoretical value of 4.51 g/cm<sup>3</sup> [10]) through adding 3 mol % excess alkali carbonates to the initial powder mixture. At sintering temperature of 1100 °C, the density decreased with increasing the excess alkali

carbonate content. This is due to an adding with high content of excess  $\text{Na}_2\text{CO}_3$  and  $\text{K}_2\text{CO}_3$  (5 mol %) showed significantly larger agglomerated cuboid particles, are potentially more difficult to mill into a sinter active powder resulting in increases its porosity. At higher sintering temperature, the presence of  $\text{Na}_2\text{CO}_3$  and  $\text{K}_2\text{CO}_3$  rich liquid phase usually helps higher densification in sintering. Further increasing of sintering temperature to 1160 °C makes too high for sintering NKN ceramics and causes the density decrease. The limiting sintered geometric density for the optimum level of excess carbonates is around 3 % lower than Archimedes density values reported for NKN ceramics made from (non-excess) powders prepared using conventional planetary milling [10]. In part this may be due to differences in measurement techniques as at these porosity levels geometric densities are often lower than corresponding values measured by water displacement.

The dependence of microstructure on the level of excess alkali carbonate and sintering temperature is shown in Figs 3-4. By using the intercept method, the average grain sizes at 1100 °C were  $4.41 \pm 2.51$ ,  $0.85 \pm 0.07$  and  $1.37 \pm 0.32$   $\mu\text{m}$  for samples with the excess alkali carbonates of 0, 1 and 3 mol%; whereas at 1140 °C they were  $4.25 \pm 0.87$ ,  $3.77 \pm 1.65$ ,  $4.07 \pm 2.25$  and  $5.56 \pm 1.09$   $\mu\text{m}$  for samples with the excess alkali carbonates of 0, 1, 3, and 5 mol%, respectively. This result showed that the grain size was strongly dependent on sintering temperature and addition of excess alkali carbonates, especially at lower sintering temperature of 1100 °C. Inhomogeneous grain was observed in non-excess NKN samples, while homogeneous and smaller in grain size was obtained for excess-sample. This is directly attributed to the addition of excess alkali carbonate suppressed grain growth with sensitive to sintering temperature. After sintering at 1140 °C, grain structure of non-excess sample was more uniform than that

of the samples contained alkali carbonates -excess. This is suggested that the higher liquid phase in excess-sample promoted an inhomogeneous grain growth at higher sintering temperature.

The dependence of dielectric property ( $\epsilon_r$  and  $\tan\delta$ ) on frequency for both of non-excess and excess-samples was investigated. It was found that the  $\epsilon_r$  and  $\tan\delta$  decreased with increase of frequency. The  $\epsilon_r$  and  $\tan\delta$  at 1 kHz as a function of amounts of excess alkali carbonates and sintering temperature at room temperature is shown in Fig 5. The amounts of excess alkali carbonates and sintering temperature were found to have a significant effect on the relative permittivity. The results showed an increase in relative permittivity up to a maximum of 1707 in the 1 mol% excess alkali carbonates contained sample. This is contributed to the more uniform and much smaller in this sample. However, at the higher alkali carbonates contained the relative permittivity decreased at lower sintering temperature (1100 °C). This result attributed to the lowering of density at the higher alkali carbonates, which causes the high porosity. The  $\epsilon_r$  decreased continuously and  $\tan\delta$  increased with increase of excess alkali carbonates content at higher sintering temperature of 1140 °C. This is due to the inhomogeneous grain structure and low densities were observed.

#### 4. Conclusions

$\text{Na}_{0.5}\text{K}_{0.5}\text{NbO}_3$  ceramics were prepared by a mixed-oxide route under various sintering conditions and amount of excess alkali carbonates starting powders. Evidence gained from XRD revealed that an orthorhombic single-phase product, with adding excess of  $\text{Na}_2\text{CO}_3$  and  $\text{K}_2\text{CO}_3$  up to 5 mol %. Maximum sintered density was achieved for 3 mol %, of the combined additive; this is attributed to an optimized liquid phase

amount to promote densification and compensation of probable alkali oxides losses. An excess-sample showed a much smaller and uniform grain size than that of non-excess sample when sintered at low temperature of 1100 °C. This is resulting in the highest relative permittivity of 1707 for 1 mol%-excess sample.

### **Acknowledgments**

This work was supported by Thailand Research Fund (TRF) and Commission on Higher Education. Thanks are given to Tom Skidmore for useful comments.

### **References**

- [1] Y. Guo, K.-I Kakimoto and H. Ohsato, Dielectric and piezoelectric properties of lead-free  $(\text{Na}_{0.5}\text{K}_{0.5})\text{NbO}_3$ - $\text{SrTiO}_3$  ceramics, Solid State Communication, 129(5) (2004) 279-284.
- [2] B. Jaffe, W. R. Cook and H. Jaffe, Piezoelectric Ceramics, Academic Press, New York, 1971.
- [3] Y. Guo, K.-I. Kakimoto and H. Ohsato,  $(\text{Na}_{0.5}\text{K}_{0.5})\text{NbO}_3$  –  $\text{LiTaO}_3$  Lead-Free Piezoelectric Ceramics, Materials Letter, 59 (2005) 241-244.
- [4] G. Shirane, R. Newnham and R. Pepinsky, Dielectric Properties and Phase Transition of  $\text{NaNbO}_3$  and  $(\text{Na}, \text{K})\text{NbO}_3$ , Phys. Rev., 96(3) (1954) 581-588.
- [5] R. Wang, R. Xie, T. Sekiya and Y. Shimojo, Fabrication and Characterization of Potassium-Sodium Niobate Piezoelectric Ceramics by Spark-Plasma Sintering Method, Mater. Res. Bull., 39 (2004) 1709-1715.
- [6] Y. Saito, H. Takao, T. Tani, T. Nonoyama, K. Takatori, T. Homma, T. Nagaya and M. Nakamura, Lead-free piezoceramics, Nature, 432 (2004) 84-87.

[7] Y. Saito and H. Takao, High performance lead-free piezoelectric ceramics in the (K<sub>x</sub>Na<sub>1-x</sub>)NbO<sub>3</sub>-LiTaO<sub>3</sub> solid solution system, *Ferroelectrics*, 338 (2006) 17-32.

[8] R.E. Jaeger and L. Egerton, Hot Pressing of Potassium-Sodium Niobates, *J. Am. Ceram. Soc.*, 45(5) (1962) 209-213.

[9] J.-F. Li, K. Wang, B.-P. Zhang and L.-M. Zhang, Ferroelectric and Piezoelectric Properties of Fine-Grained Na<sub>0.5</sub>K<sub>0.5</sub>NbO<sub>3</sub> Lead-Free Piezoelectric Ceramics Prepared by Spark Plasma Sintering, *J. Am. Ceram. Soc.*, 89(2) (2006) 706-709.

[10] R. Zuo, J. Rödel, R. Chen and L. Li, Sintering and Electrical Properties of Lead-Free Na<sub>0.5</sub>K<sub>0.5</sub>NbO<sub>3</sub> Piezoelectric Ceramics, *J. Am. Ceram. Soc.*, 89(6) (2006) 2010-2015.

[11] H. Birol, D. Damjanovic and N. Setter, Preparation and Characterization of KNbO<sub>3</sub> Ceramics, *J. Am. Ceram. Soc.*, 88(7) (2005) 1754-1759.

[12] E. Hollenstein, M. Davis, D. Damjanovic and N. Setter, Piezoelectric Properties of Li- and Ta-Modified (K<sub>0.5</sub>Na<sub>0.5</sub>)NbO<sub>3</sub> Ceramics, *Appl. Phys. Lett.*, 87 (2005) 1-3.

[13] D. R. Lide, *Handbook of Chemistry and Physics*, 74<sup>th</sup> Edition, CRC- Press, 1993.

[14] V. Lingwal, B. S. Semwal and N. S. Panwar, Dielectric Properties of Na<sub>1-x</sub>K<sub>x</sub>NbO<sub>3</sub> in Orthorhombic Phase, *Bull. Mater. Sci.*, 26(6) (2003) 619-625.

[15] Powder Diffraction File No. 32 – 0822, International Centre for Diffraction Data, Newton Squire, PA, 2001.

## List of Figures

**Figure 1** X-ray diffraction (XRD) patterns of samples with different amount of alkali carbonates when sintered at 1140 °C

**Figure 2** The density of samples with different amount of alkali carbonates and sintering temperatures.

**Figure 3** SEM micrographs of samples with different amount of alkali carbonates when sintered at 1100 °C; (a) Non-excess, (b) 0.01 mol and (c) 0.03 mol.

**Figure 4** SEM micrographs of samples with different amount of alkali carbonates when sintered at 1140 °C; (a) Non-excess, (b) 0.01 mol, (c) 0.03 mol and (d) 0.05 mol.

**Figure 5** The dielectric property of samples with different amount of alkali carbonates and sintering temperatures; (a) relative permittivity and (b)  $\tan \delta$  at 1 kHz.

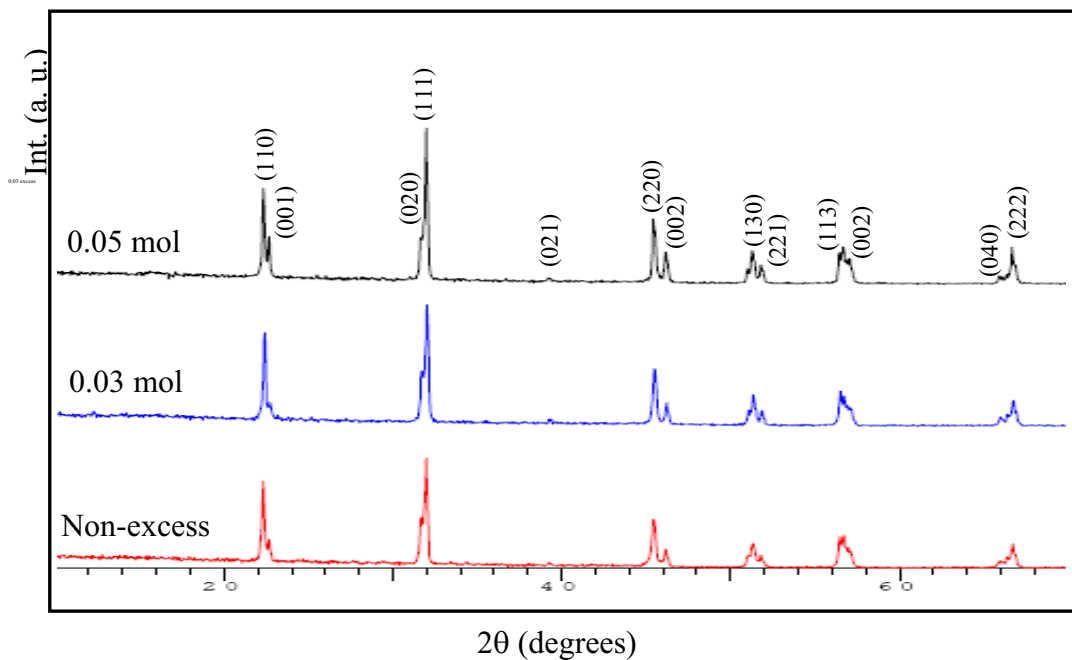


**Figure 1** X-ray diffraction (XRD) patterns of samples with different amount of alkali carbonates when sintered at 1140 °C. The orthorhombic pattern is indexed according to JCPDS data file no. 32-0822 [15].

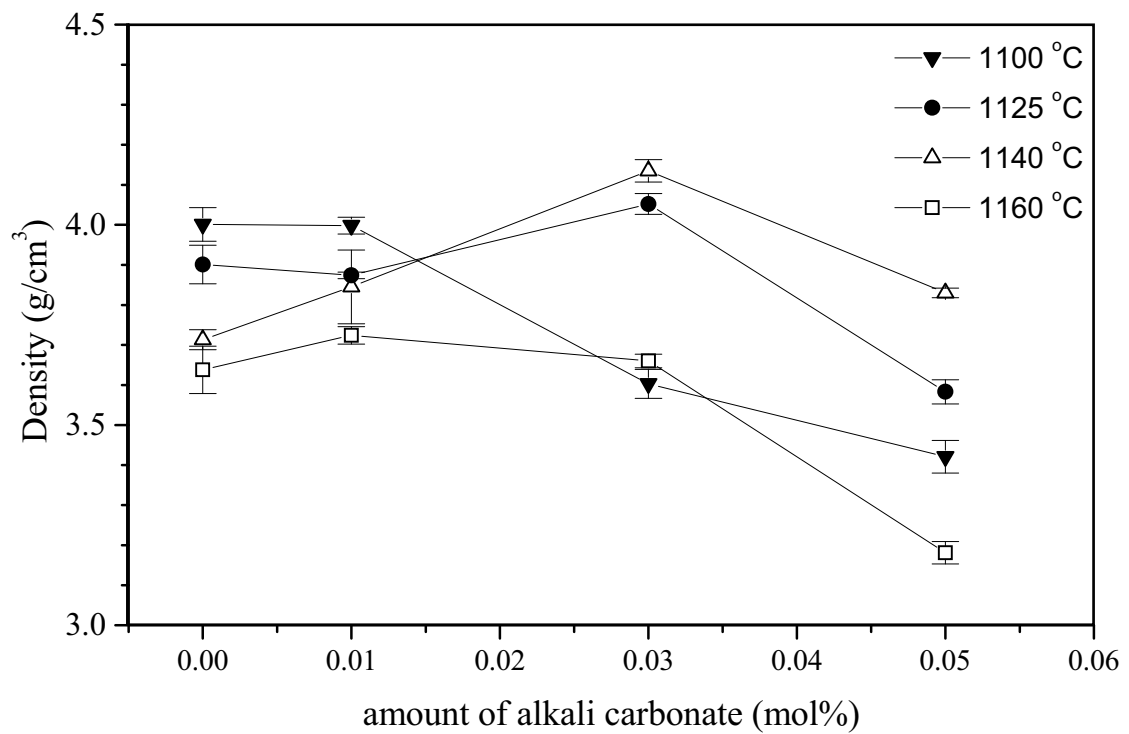


Figure 2 The density of samples with different amount of alkali carbonates and sintering temperatures.

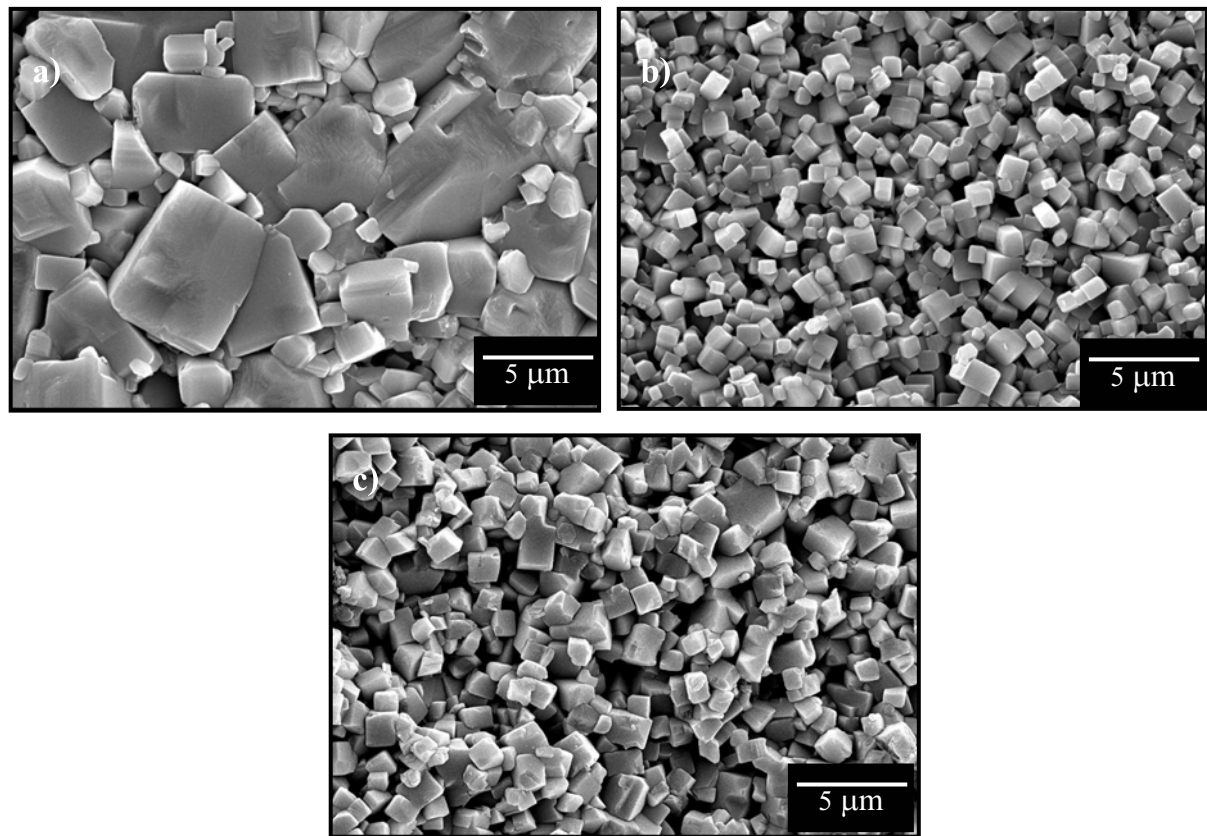


Figure 3 SEM micrographs of samples with different amount of alkali carbonates when sintered at 1100 °C; (a) Non-excess, (b) 0.01 mol and (c) 0.03 mol.

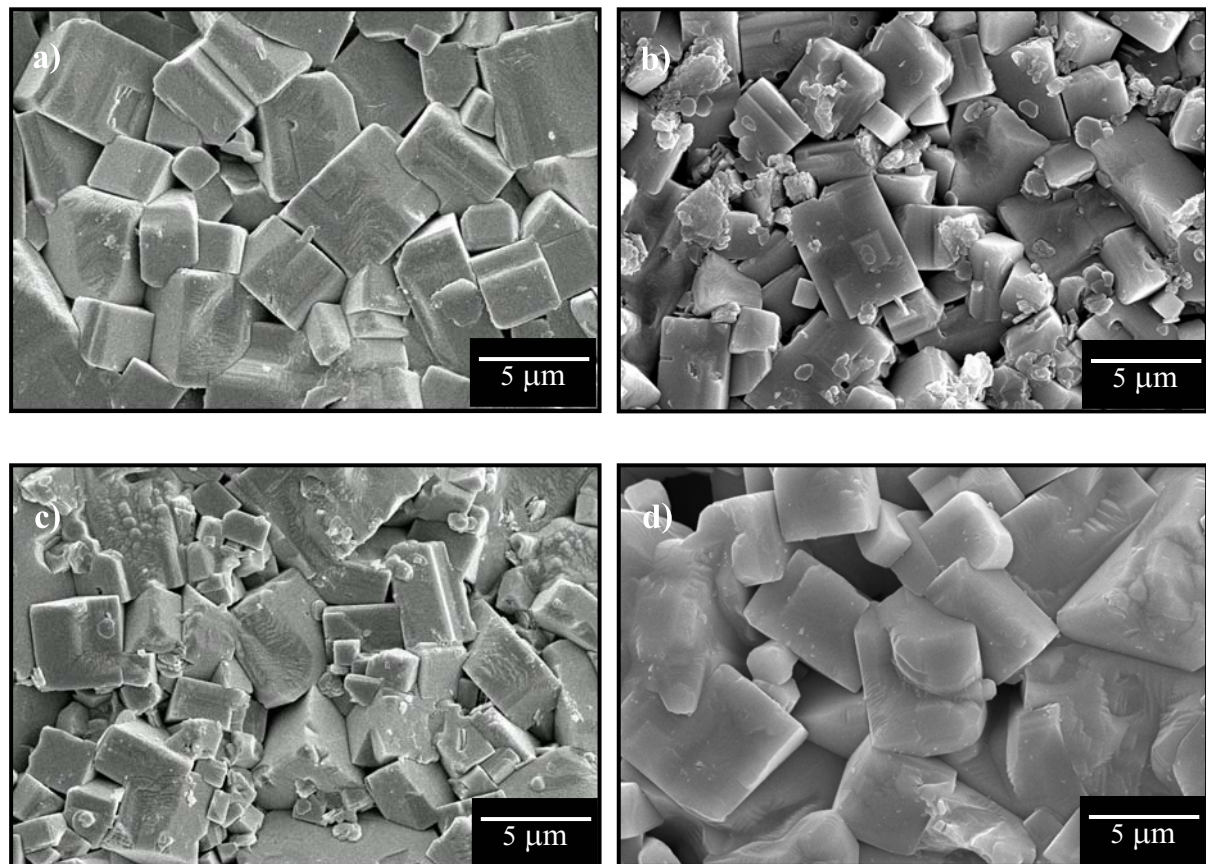


Figure 4 SEM micrographs of samples with different amount of alkali carbonates when sintered at 1140 °C; (a) Non-excess, (b) 0.01 mol, (c) 0.03 mol and (d) 0.05 mol.

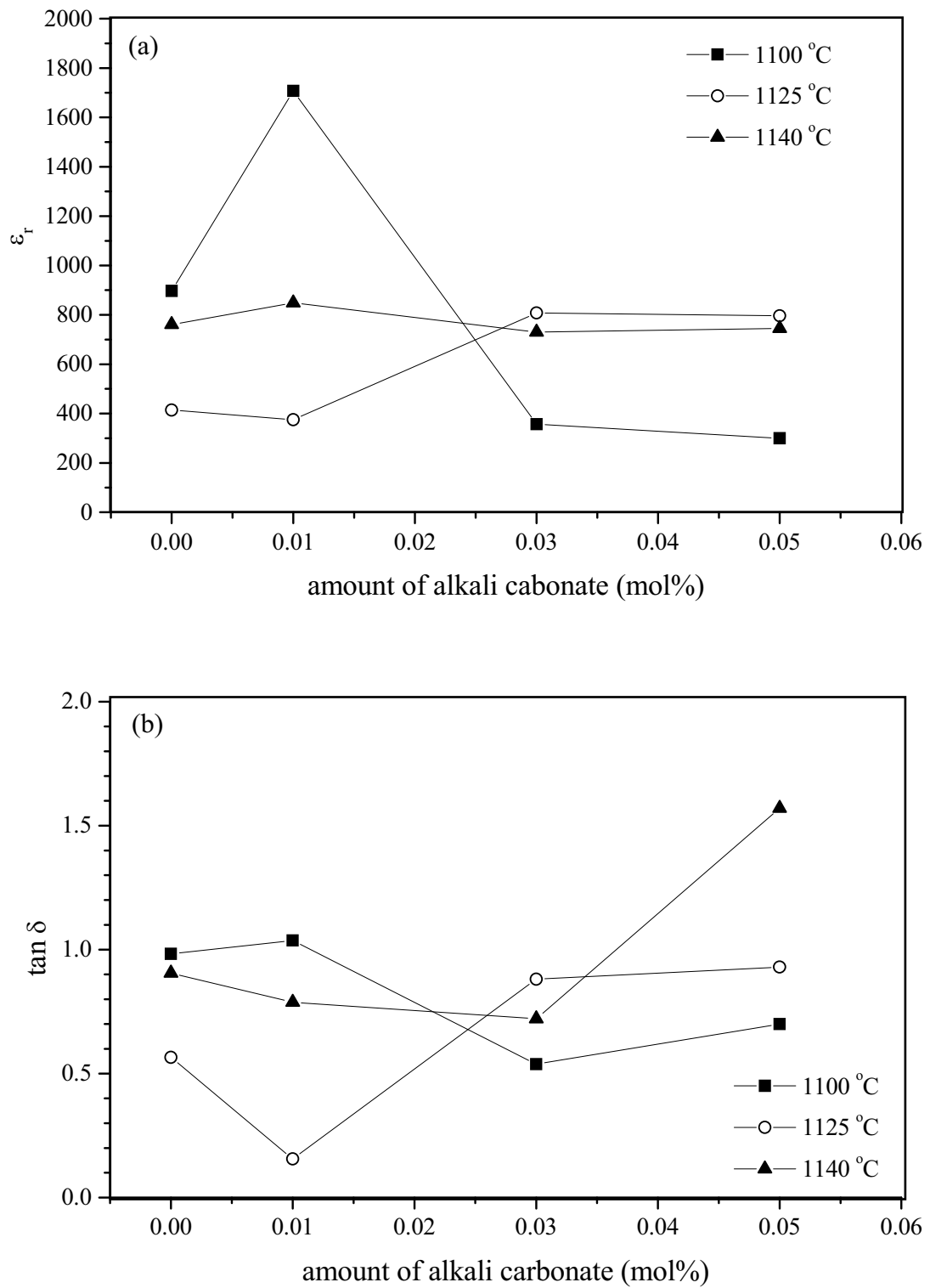


Figure 5 The dielectric property of samples with different amount of alkali carbonates and sintering temperatures; (a) relative permittivity and (b)  $\tan \delta$  at 1 kHz.

# **Phase Development, Densification and Dielectric Properties of (0.95-x)Na<sub>0.5</sub>K<sub>0.5</sub>NbO<sub>3</sub> - 0.05LiTaO<sub>3</sub> - x LiSbO<sub>3</sub> Lead-free Piezoelectric Ceramics**

**Pornsuda Bomlai<sup>1,\*</sup>, Sureewan Sukprasert<sup>1</sup>, Supasarute Muensit<sup>2</sup> and  
Steven J. Milne<sup>3</sup>**

<sup>1</sup>*Materials Science Program, and <sup>2</sup>Department of Physics, Faculty of Science,  
Prince of Songkla University, Songkla 90112 Thailand*

<sup>3</sup>*Institute for Materials Research, University of Leeds, Leeds LS2 9JT,  
United Kingdom.*

## **Abstracts**

Lead-free piezoelectric ceramics in the system (0.95-x)Na<sub>0.5</sub>K<sub>0.5</sub>NbO<sub>3</sub> - 0.05LiTaO<sub>3</sub> - xLiSbO<sub>3</sub>, x = 0-0.1, were synthesized by a reaction-sintering method. The effects of the content of LiSbO<sub>3</sub>, and the sintering temperature on phase-development, microstructure and dielectric properties of the samples were investigated. Additions of LiSbO<sub>3</sub> produced a change in crystal system from orthorhombic to tetragonal. The additive reduced the temperature at which secondary recrystallisation occurred, and also affected average grain size, and dielectric constant. A sintering temperature of 1050 °C (for 2h) was the optimum for this system in order to achieve a high density and high dielectric constant. A maximum dielectric constant of 1510 was recorded for the x = 0.04 composition.

**KEYWORDS:** A. ceramics, B. crystal structure, C. X-ray diffraction, D. dielectric properties, D. microstructure.

*\* Corresponding e-mail: ppornsuda@yahoo.com*  
Tel. +66 74 288 250; Fax +66 74 218 701.

## 1. Introduction

Environmental concerns are stimulating research into the development of lead-free alternative piezoelectric ceramics [1-2]. Mixed alkali niobate-tantalates are leading candidates as replacements for lead zirconate titanate, PZT.

Guo *et al.*[3] investigated the alkali niobate solid solution system  $[\text{Na}_{0.5}\text{K}_{0.5}\text{NbO}_3]_{1-x} - [\text{LiTaO}_3]_x$  (abbreviated, NKN-LT) and reported a morphotropic phase boundary (MPB), at  $0.05 < x < 0.06$ , between orthorhombic and tetragonal phase-fields. Compositions close to this MPB gave the highest values of  $d_{33}$  piezoelectric charge coefficients in the system, reaching a value of  $\sim 200 \text{ pC/N}$  at  $x = 0.05$  with a corresponding Curie temperature ( $T_c$ ) of  $\sim 420 \text{ }^\circ\text{C}$ .

Saito *et al.* [4-5] studied a wider range of related solid solutions, corresponding to the general formula  $(\text{K}_{0.5}\text{Na}_{0.5})_{1-x}\text{Li}_x\text{Nb}_{1-y}\text{Ta}_y\text{O}_3$ . For a composition,  $x = 0.03$  and  $y = 0.2$ , close to the MPB of this system,  $d_{33}$  was  $230 \text{ pC/N}$ , with a  $T_c$  of  $323 \text{ }^\circ\text{C}$ . Reactive template grain growth resulted in enhanced piezoelectric properties, giving values of  $d_{33} = 373 \text{ pC/N}$  and  $T_c = 323 \text{ }^\circ\text{C}$  for  $\langle 001 \rangle$  grain-oriented ceramics. Slightly improved values of  $d_{33}$  coefficients were obtained using Sb ion doping on the pentavalent sites of the perovskite lattice. These values approach those of some PZT ceramics and consequently have aroused keen interest in developing this compositional system further as a viable Pb-free piezoceramic [6-11].

Although the highest piezoelectric coefficients were demonstrated for textured ceramics fabricated using reactive template grain growth, these fabrication procedures are rather complicated and would be costly for commercial production. Hence it is important to optimize properties in conventional, randomly orientated ceramic samples. For example, Marcos *et al.* [12] have used conventional ceramic processing techniques to

fabricate ceramics of  $(K_{0.44}Na_{0.52}Li_{0.04})(Nb_{0.86}Ta_{0.10}Sb_{0.04})O_3$ , a composition in the system reported by Saito et al. [4], and also a ‘non-stoichiometric’ composition  $(K_{0.38}Na_{0.52}Li_{0.04})(Nb_{0.86}Ta_{0.10}Sb_{0.04})O_{2.97}$ . A higher piezoelectric coefficient was obtained for the latter, with  $d_{33} \sim 200$  pC/N.

The present paper addresses phase development, ceramic densification, microstructural evolution and dielectric properties in compositions expressed by the general formula  $(0.95-x)Na_{0.5}K_{0.5}NbO_3-0.05LiTaO_3-xLiSbO_3$ , made by a mixed-oxide processing route, employing reaction-sintering. The end-member composition,  $0.95(Na_{0.5}K_{0.5}NbO_3)-0.05LiTaO_3$  lies near the MPB in the base NKN-LT system.

## 2. Experimental procedure

Samples were prepared by the conventional mixed-oxide process using  $K_2CO_3$ ,  $Ta_2O_5$  (Aldrich Chemical Company, Inc.,  $\geq 99.0\%$  purity),  $Na_2CO_3$ ,  $Nb_2O_5$  (Aldrich Chemical Company, Inc.,  $99.9+\%$  purity),  $Li_2CO_3$  (Fluka,  $>99.0\%$  purity) and  $Sb_2O_5$  (Aldrich Chemical Company, Inc.,  $99.995\%$  purity), as starting powders. The stoichiometric  $Na_{0.5}K_{0.5}NbO_3$  powder was firstly prepared for this system. The two carbonate powders are moisture-sensitive; thermogravimetric analysis indicates that dehydration is completed at  $\sim 200$  °C, therefore to avoid compositional errors when weighing out the  $Na_{0.5}K_{0.5}NbO_3$  precursor mixture, the starting reagents were dried in an oven for 24 h prior to use. Dried powders were allowed to cool to room temperature under reduced pressure in a dessicator, and all powders were stored in the dessicator until immediately prior to weighing in the correct proportions. The starting materials were transferred to a 100 mm-diameter cylindrical plastic jar, partially filled with 10 mm-diameter alumina grinding balls. Sufficient ethanol was added to cover the powder/media.

Ball-milling was carried out for 24 h, followed by drying at 120 °C, prior to grinding with an alumina mortar and pestle to break up large agglomerates formed during drying. The mixtures were calcined in alumina crucibles, with loosely fitting lids, at 800 °C for 2 h. The NKN powders were then ground, weighed and ball-milled again for 24 h with  $Ta_2O_5$ ,  $Li_2CO_3$  (dried) and  $Sb_2O_5$  to obtain the compositions  $(0.95-x)Na_{0.5}K_{0.5}NbO_3 - 0.05LiTaO_3 - x LiSbO_3$  (abbreviated as NKN-LT-LS) for  $x = 0.0, 0.02, 0.04, 0.06$  and  $0.10$ . A reaction-sintering approach was used to produce the NKN-LT-LS ceramics, in that no second powder calcination stage was employed prior to sintering. The mixed powders were dried, ground and pressed at 100 MPa into 1.5 cm diameter discs and sintered in air at temperature ranging from 1025 - 1150°C for 2 h in closed crucibles.

Ceramic samples were examined at room temperature using X-ray powder diffraction (XRD; Philips X' Pert MPD, Ni-filtered  $CuK\alpha$  radiation) to identify the phase(s) formed. Sintered pellet densities were obtained by the Archimedes method. The microstructures of the as-sintered surfaces of the samples were imaged directly, using scanning electron microscopy (SEM; Jeol : JSM-5800LV). The average grain size was calculated by the mean linear intercept method. To investigate dielectric properties, pellets were electrode with silver paste (SPI Supplies) and capacitance and loss tangents ( $\tan \delta$ ) of the samples measured at room temperature using a LCR meter (HP 4263B) at 1 kHz, from which the dielectric constant was calculated.

### **3. Results and discussion**

Figure 1 shows XRD patterns of the  $(0.95-x)Na_{0.5}K_{0.5}NbO_3 - 0.05LiTaO_3 - x LiSbO_3$  samples which had been sintered at 1050 °C for 2 h. It was found that the phase structure of the product depended significantly on the addition of  $LiSbO_3$ . Perovskite

phase was formed in high yield in all samples, but secondary phases appeared. An extra phase, giving faint peaks with a similar pattern to  $K_6Li_4Nb_{10}O_{30}$  [13], was detected in all compositions, Fig 1. Residual  $LiSbO_3$  [14] was detected in the  $x = 0.10$  sample, Fig1. Further phase analysis was conducted with reference to XRD patterns of a single-phase orthorhombic material (NKN), and of a tetragonal pattern of a 0.94NKN-0.06LT composition, as shown in Figure 3 [15-16]. For the orthorhombic perovskite phase the lower angle peak in the 45-46.5  $^{\circ}2\theta$  pair (highlighted for the  $x = 0$  and 0.04 compositions in Figure 2) is the most intense, whilst the reverse holds true for the tetragonal phase. These peaks correspond to (022) and (002) peaks for the orthorhombic phase, and (002) and (200) peaks for the tetragonal phase. Figures 1 and 2 thus indicate the main product phase for the  $x = 0$  composition,  $0.95Na_{0.5}K_{0.5}NbO_3-0.05LiTaO_3$ , to be orthorhombic [3], while all samples with added  $LiSbO_3$ ,  $x = 0.02 - 0.10$ , showed a tetragonal perovskite solid solution [5]. There was a slight increase in d-spacing between  $x = 0$  and  $x = 0.02$  samples, for example from 1.994  $\text{\AA}$  to 2.010  $\text{\AA}$ , for the orthorhombic 022 and tetragonal 002 peaks respectively, Table 1 and Fig 2. However no significant variation in d-spacings were detected for compositions,  $x = 0.02-0.1$ .

Calculation of the respective peak intensity ratio within the 45-46.5  $^{\circ}2\theta$  pair of peaks (calculated from peak heights) for an orthorhombic NKN ‘standard’ pattern gives a  $I_{022}/I_{002}$  value of  $\sim 1.3$  [15], whilst  $I_{002}/I_{200}$  is  $\sim 0.5$  for the ‘standard’ tetragonal phase [16]. In the present ceramics sintered at 1050  $^{\circ}\text{C}$ , the characteristic XRD pattern of the  $x = 0$  composition, gives a peak ratio ( $I_{022}/I_{002}$ ) of  $\sim 1.4$ , whereas the  $LiSbO_3$  modified samples have corresponding values ( $I_{002}/I_{200}$ ) of  $\sim 0.6-0.8$ , Table 1. Although structure factor differences between NKN-LT and NKN-LT-LS solid solutions and those of the selected reference materials will influence specific values, the reference materials

nevertheless provide a basis from which to evaluate the phase content of the experimental samples in detail. The comparative values illustrate that the main product phase for  $x = 0$  is solely the orthorhombic NKN-LT phase. However although the  $\text{LiSbO}_3$  modification induces a stabilization of the tetragonal polymorph, the actual values of peak ratios (0.6-0.8) are somewhat higher, in relative terms, than for the reference tetragonal pattern (0.5). This suggests that after sintering at 1050 °C for 2 h there may be some coexisting orthorhombic material along with the predominant tetragonal phase. The net result is a slight increase in intensity ratio from the base tetragonal value of 0.5.

Increasing the sintering temperature to 1075 °C brought the experimental intensity ratios closer to the values expected from single- phase tetragonal systems for  $x = 0.02-0.1$ . However there was still a very small amount of  $\text{LiSbO}_3$  second phase present in  $x = 0.1$ , and a small amount of the second phase  $\text{K}_6\text{Li}_4\text{Nb}_{10}\text{O}_{30}$  – type structure in all compositions.

A major change in phase content occurred at the highest sintering temperature investigated, 1150 °C, Figs 2 and 4. The tetragonal pattern was replaced by a pattern similar to that of cubic perovskite. This probably is indicative of partial melting occurring at 1150 °C.

The variation in densities of the  $(0.95-x)\text{Na}_{0.5}\text{K}_{0.5}\text{NbO}_3-0.05\text{LiTaO}_3-x\text{LiSbO}_3$  ceramics for different sintering temperatures, is shown in Fig 5. It was found that density was very sensitive to slight changes in sintering temperature. The highest density samples were produced at a sintering temperature of 1050 °C. This is around 50 °C lower than required for ceramics of related compositions prepared by full calcination prior to sintering [16], indicating the effectiveness of the reaction sintering approach. Density values were  $4.32 \pm 0.01 \text{ g/cm}^3$  for a sample with  $x = 0.0$ , increasing gradually with

increasing amounts of  $\text{LiSbO}_3$  giving a value of  $4.44 \pm 0.01 \text{ g/cm}^3$  for a sample with  $x = 0.10$ . This trend may reflect the higher mass of Sb. Indeed recalling that some  $\text{LiSbO}_3$  was detected in the  $x = 0.1$  sample at  $1050^\circ\text{C}$ , the higher density of  $\text{LiSbO}_3$  ( $\sim 5.45 \text{ g/cm}^3$ ) will increase the measured density of this sample, Fig 5. At  $1075^\circ\text{C}$ , the ceramic densities were  $\sim 2\%$  lower than at  $1050^\circ\text{C}$ ; this trend generally continued with further  $25^\circ\text{C}$  increments in sintering temperature, Fig 5. However for the highest  $\text{LiSbO}_3$  samples,  $x = 0.1$ , and to a lesser extent,  $x = 0.06$ , the density fell more rapidly with rising sintering temperature. This is attributed to structural changes, and possible melting (Figure 5). For all sample compositions, an increase in volatilisation losses, particularly of Li and K [16] and possibly Sb at temperatures  $> 1050^\circ\text{C}$  may contribute to the observed gradual decrease in measured densities with increasing temperature

The microstructures of samples sintered at temperatures ranging from  $1050 - 1100^\circ\text{C}$  showed that grain size and shape depended strongly on sintering temperature and on  $\text{LiSbO}_3$  content, Figs 6-8. For a sintering temperature of  $1050^\circ\text{C}$ , the  $x = 0$  and  $x = 0.02$  compositions each showed grain sizes  $< 1 \mu\text{m}$ , however at  $x = 0.04$  a change to much larger maximum grain sizes, and a distribution typical of secondary recrystallisation was evident, Fig 6. This mechanism produced cuboid grains with maximum grain sizes  $\sim 5 \mu\text{m}$  in a fine grained matrix, Fig 6c,d.

At  $1075^\circ\text{C}$  all compositions,  $x = 0.02-0.1$ , showed secondary recrystallisation. Maximum grain sizes were  $\sim 8 \mu\text{m}$  for  $x = 0$ . A slight decrease in grain size was observed with increasing  $\text{LiSbO}_3$  content. Sintering at  $1100^\circ\text{C}$  produced a maximum grain size of  $\sim 12 \mu\text{m}$  in the  $x = 0$  sample. Again the trend of decreasing grain size with increasing  $\text{LiSbO}_3$  substitution was observed.

Variations in *average* grain size, as calculated by the linear intercept method, are shown in Fig 9. There was a marked discontinuity in the 1050 °C plot between  $x = 0.02$  and  $0.04$  due to the change in grain growth mechanism. A gradual decrease in average size with increasing  $x$  is evident for higher sintering temperatures, where all compositions exhibit secondary recrystallisation.

In other perovskites such as  $\text{BaTiO}_3$ , secondary recrystallisation is often thought to be associated with liquid phase formation. A similar mechanism leading to bimodal grain size distributions may occur in the NKN-LT-LS system. Changes in microstructure with increasing temperature, and increasing  $\text{LiSbO}_3$  content, may relate to changes in the amount and composition of any liquid phase.

Dielectric properties of dense samples, sintered at temperatures ranging from 1050 – 1100 °C, are shown in Fig 10. The dielectric constant of the  $x = 0$ , NKN sample was  $\sim 600$ -700 for the full range of sintering temperatures studied, 1050-1100 °C. This value is higher than that reported in previous studies for  $0.95\text{Na}_{0.5}\text{K}_{0.5}\text{NbO}_3\text{-}0.05\text{LiTaO}_3$  [17] or for NKN ceramics sintered at 1110 °C [3].

The incorporation of  $\text{LiSbO}_3$  brought about substantial increases in the dielectric constant. Values were a maximum of 1510 for the  $x = 0.04$  starting composition, sintered at 1050 °C, Fig 10. Values for  $x = 0.02$  and  $0.06$  were also relatively high, 1300-1350, for this sintering temperature, but the  $x = 0.1$  sample had a much lower value, similar to that of  $x = 0$ . The latter effect may be due to the presence of unreacted  $\text{LiSbO}_3$ . A dielectric constant of 1510 for  $x = 0.04$  is very close to that reported for textured ceramics of  $(\text{K}_{0.44}\text{Na}_{0.52}\text{Li}_{0.04})(\text{Nb}_{0.86}\text{Ta}_{0.10}\text{Sb}_{0.04})\text{O}_3$  for which the value reached 1570 [4], and is much higher than values reported for alkali niobate tantalate (NKN-LT) compositions produced by conventional calcination and sintering [3, 7].

Sintering at higher temperatures, 1075 °C or 1100 °C produced lower dielectric constants than for the 1050 °C samples, which may relate to their lower densities. For all compositions, the value was between ~ 800-1000. Dissipation factors for the LiSbO<sub>3</sub> - modified samples were higher than expected, varying between ~ 0.1-0.7. The highest value occurred for the x = 0.04 sample sintered at 1050 °C. One possible reason for the high dissipation factors may be a high electrical conductivity, which could be related to alkali oxide (or antimony oxide) losses during sintering. However oxide volatilisation would increase with increasing sintering temperature, yet the dissipation factors were lower, ~ 0.5, for the x = 0.04 ceramics sintered at 1075 °C and 1100 °C.

#### 4. Conclusions

Small increments to sintering temperature, and changes to the amount of LiSbO<sub>3</sub> strongly affect phase content, densification, microstructure and dielectric properties of (0.95-x)Na<sub>0.5</sub>K<sub>0.5</sub>NbO<sub>3</sub>-0.05LiTaO<sub>3</sub>-xLiSbO<sub>3</sub> ceramics. The additive promotes the formation of a tetragonal crystal structure, as opposed to the orthorhombic structure of the 0.95Na<sub>0.5</sub>K<sub>0.5</sub>NbO<sub>3</sub>-0.05LiTaO<sub>3</sub> end-member. The reaction-sintering approach employed produces maximum densities of 4.3-4.4 g/cm<sup>3</sup> for a sintering temperature of only 1050 °C. This is a lower temperature than is usually reported for ceramics of related compositions fabricated using full powder calcination before sintering. A composition 0.91(Na<sub>0.5</sub>K<sub>0.5</sub>)NbO<sub>3</sub> - 0.05LiTaO<sub>3</sub> – 0.04LiSbO<sub>3</sub> sintered at 1050 °C shows the highest dielectric constant in this system, with a room –temperature value of ~1510. Raising the sintering temperature from 1050 °C to 1075 °C, produced ceramics with ~ 2 % lower density and dielectric constants were reduced in value to ~ 1000.